

When are D-graded neighborhoods not degraded? Greening the legacy of redlining

Alba Miñano Mañero*

CEMFI

November 2022

ABSTRACT: This paper explores how geography shapes the long-term effects of historic redlining policies. Comparing neighborhoods deprived of credit by the US Federal government, D-graded, with adjacent C-graded ones –subject to a less stringent policy– shows that four decades after the outlawing of redlining, gaps in home values, income, and racial composition are less prevalent in D-graded areas near the coast or a park. To understand the sources of faster convergence, we assemble for all cities of interest a geo-located inventory of waterfront modifications, a novel panel of tree coverage constructed by applying machine learning to historical imagery and current near-infrared images, and an instrument for changes in tree canopy exploiting tree replacements due to geographic variation in tree plagues and susceptible species. Results show that improvements in abandoned waterfronts and expansions in tree coverage drive the faster convergence.

Key words: redlining, geography

JEL classification: R23

*I am grateful to my advisor, Diego Puga, for all his guidance and help. I also thank Elisabet Viladecans-Marsal, Paula Bustos, Dmitry Arkhangelsky, Jorge de la Roca, Monica Martinez-Bravo and attendants to BUDIE, Cemfi PhD Workshops and the UEA Summer School in Urban Economics for all their valuable comments and suggestions. I am likewise indebted to Cayrua Chaves for all his help automatizing the imagery download process. I gratefully acknowledge funding from Spain's State Research Agency through its María de Maeztu Units of Excellence programme (MDM-2016-0684).

"To a great extent in postwar America, geography is destiny"

— Thomas Sugrue, *The Origins of the Urban Crisis: Race and Inequality in Postwar Detroit*.

1. Introduction

Redlining in housing markets is one of the sharpest cases of institutionalized racial discrimination in the United States. After having outlawed discriminatory laws, the legacy of these institutional racist practices is still behind the racial component of current inequality (Rothstein, 2017). Policies that degrade neighborhoods restrict access to high-opportunity locations while lowering the value of people's primary source of wealth, housing. Because neighborhood change is a medium-to-long-run phenomenon, their inequalities can persist longer.

Despite growing research on the legacy of redlining, neighborhoods' differences in intrinsic factors as geography have gone unnoticed. Heterogeneity in fundamental neighborhood characteristics implies that the legacy of redlining varies depending on these features. If these fundamental local components are modifiable, potential interventions could reverse the effects on neighborhoods, but not necessarily on their inhabitants. This paper focuses on how geography and its modifications can mediate the persistence of redlining.

Foreclosures became so prevalent after the Great Depression that the Federal government began insuring mortgages through the Home Owners' Loan Corporation (HOLC) in 1933 and the Federal Housing Administration (FHA) from 1934. Both institutions facilitated a rapid expansion of credit and home ownership in the United States, but followed lending guidelines that led to sharp discrimination in housing markets. In particular, the HOLC developed an appraisal system that graded neighborhoods from A to D, and deemed areas in the worst two grades too risky for investment. The racial composition of each area was decisive in determining its grade, and D-graded neighborhoods were systematically those with very high shares of African-Americans. The assessment process was reflected in the creation of colour-coded maps, where D-graded areas were painted in red, leading to the term redlining, used to refer to systematic credit denials based on neighborhood characteristics. By institutionalising the discriminatory practices of realtors and lenders against African Americans, redlining lowered home ownership amongst them and strengthened racial segregation.

The evidence of Fishback, Rose, Snowden, and Storrs (2022) challenges the HOLC maps' relevance as the determinant in the implemented redlining practices. The validity of the results based on the HOLC maps would be jeopardized if active lending actors used different maps to guide their decisions. The HOLC maps reflected the prevailing appraisal guidelines of America at that period, since the HOLC and local brokers jointly developed them. As a result, regardless of the diffusion of the HOLC maps, they remain the best approximation to the discriminatory lending practices of the time.

Recent research has focused on providing causal estimates of the persistence of the HOLC maps and addressed the concern that the assigned grades reflected previous differences in

the socioeconomic composition and housing characteristics of neighborhoods by comparing nearby areas with similar features but different grades (Appel and Nickerson (2016); Krimmel (2018) and Aaronson, Hartley, and Mazumder (2021b)). This paper develops a novel method for creating data at the original HOLC neighborhood level to implement a similar empirical diff-in-diff strategy that compares D-graded areas, subject to the most severe credit restriction, to nearby areas subject to a less restrictive credit policy (C-graded, yellowlined). Consistent with the literature, results show that the legacy of redlining persists after its formal outlawing.

Other unconnected literature highlights that natural amenities are fundamental for neighborhood outcomes (Rappaport and Sachs (2003); Rappaport (2007); Villarreal (2014); Lee and Lin (2018); Heblitch, Trew, and Zylberberg (2021)). As a result, the effects of redlining should not be the same in all neighborhoods. This possibility, however, had been neglected by previous research. Incorporating natural amenities reveals that the persistence of redlining is highly heterogeneous and that geography plays an important role: convergence in demographics and housing values is higher in D areas near water and park natural amenities.

Showing that waterfront beautifications and vegetation are effective ways to modify natural amenities and revert the legacy of redlining represents a departure from the traditional idea of geography as destiny in the literature. Results imply that the waterfront revitalization projects in abandoned industrial areas are the drivers of the observed faster convergence in areas near water and parks.

This paper also implements a novel method to predict exogenous changes in urban tree coverage: tree replacements caused by changes in exposure to non-native tree plagues. The interplay between plague response policies and tree ordinances motivates the instrumentation approach. The minimum plague management strategy includes the removal of hosts, including healthy ones (Aukema, Leung, Kovacs, Chivers, Britton, Englin, Frankel, Haight, Holmes, Liebhold, et al. (2011); Hudgins, Koch, Ambrose, and Leung (2022)), but city regulations establish that removed trees ought to be replaced in different proportions depending on tree characteristics. The implication is that geographic variation in tree plagues entails exogenous variation in increases in tree coverage that can be captured in a variable that contains the length of exposure to tree pests and their potential host distribution. Both elements reflect the intensity of the response to the outbreaks, as more affected areas will be those where more trees are susceptible to being infested, where trees have been exposed for longer periods, and where the growing stage of the newly planted trees is advanced enough for tree detection algorithms to identify it. The findings reveal that exogenous increases in tree canopy can close the population and income D-C gaps, but they are also associated with gentrification and worse outcomes for the black population. This final result implies that modifications of natural amenities may be effective ways to revert the consequences of redlining for neighborhoods, but not for the originally discriminated communities.

This work is related to the literature on redlining following the digitization of the HOLC

maps (Nelson, Winling, Marciano, Connolly, et al., 2017)¹. While a strand of this literature has focused on developing new estimation strategies to estimate the causal effect of redlining, as Aaronson et al. (2021b) or Hynsjö and Perdoni (2022), another strand has directly exploited the D-C bordering grade discontinuities, as Appel and Nickerson (2016) and Krimmel (2018). The bordering differencing strategies followed by both approaches require observing sharp changes in credit restrictions but gradual changes in unobserved characteristics. Due to the misalignment between original HOLC maps and Census units, assigning grades to Census areas challenges the requirement by erasing the sharp variation needed and inducing measurement error. The methodological contribution to this literature is developing a new data creation process that satisfies the requirements of the differencing strategy. Data is created by assigning Census units to the neighborhood drawn by the HOLC with the development of the Census-to-Redlining Constant Crosswalks. The crosswalks preserve the original variation in grade assignments and guarantee gradual changes at the border by apportioning Census units to neighborhoods. Linking the heterogeneous persistence of redlining to the presence of natural amenities contributes to the research on redlining but also to the one focusing on the role of natural amenities as determinants of neighborhood trajectories (Rappaport and Sachs (2003); Rappaport (2007); Villarreal (2014); Lee and Lin (2018); Heblitch et al. (2021)).

The introduction of modifications of natural amenities constitutes two distinct contributions. The notion that geography changes with waterfront beautification projects or that natural amenities can be created in areas without them with tree coverage is a conceptual contribution to this literature that regards geography as immutable. The second contribution relates to the construction of the modification data. This paper presents a new data set containing the geographic location and date of modification projects of abandoned waterfronts in the cities under study. Although research noticed how technological changes in industry and commerce affected the role of water natural amenities in American cities (see Jackson (1987) or Boustan, Bunten, and Hearey (2018)), this idea had not been formally explored yet. Moreover, it develops a new methodology to construct panels of tree coverage modifying machine learning algorithms to predict trees in older aerial images using current training data (Yang, Wu, Praun, and Ma (2009) and Bosch (2020)). Considering tree coverage as a natural amenity and an intervention to overcome the inequalities provoked by decades of credit restrictions also contributes to recent studies that have focused on present urban tree inequality as an outcome of past redlining policies (Namin, Xu, Zhou, and Beyer (2020); Nardone, Rudolph, Morello-Frosch, and Casey (2021); Locke, Hall, Grove, et al. (2021)). The proposed instrumentation strategy to tackle endogeneity in tree coverage adds to the extensive literature exploring the impact of urban

¹The discovery of the maps by Kenneth Jackson in the 80s was followed by a small set of city studies that explored the relationship between D-graded areas and credit access and the determinants of the assigned grades (Hillier (2003) and Hillier (2005) focusing on Philadelphia, Crossney and Bartelt (2005)'s study of Philadelphia and Pittsburgh and Fishback (2014) on New York). However, the lack of availability of digitized maps at a large scale prevented the research from increasing its geographic and timing scope.

trees on economic, social, and environmental outcomes² since few papers have dealt with this issue (Wachter and Wong (2008); Kondo et al. (2017); Han, Heblitch, Timmins, and Zylberberg (2021)). In contrast to Kondo et al. (2017) and Han et al. (2021) that use a specific plague in a particular city and exploit variation in tree mortality, the instrument used in this paper relies on a different source of exogenous variation: the increases in tree coverage associated to replacements induced by the most deadly tree plagues defined in Fei, Morin, Oswalt, and Liebhold (2019).

This work is also related to other bodies of research. Analyzing the effects of local credit access connects to the strand of the literature that studies the impact of similar local policies, as research focused on zoning restrictions (Ihlfeldt (2007); Shertzer, Twinam, and Walsh (2016); Twinam (2017); Twinam (2018); Shertzer, Twinam, and Walsh (2018)). More broadly, this paper is also related to the literature on location fundamentals and persistence of urban structure (Davis and Weinstein (2002); Brakman, Garretsen, and Schramm (2004); Miguel and Roland (2011); Bleakley and Lin (2012); Ahlfeldt, Redding, Sturm, and Wolf (2015); Cuberes and González-Val (2017); Ambrus, Field, and Gonzalez (2020)). Lastly, exploring the link between credit access and modifiable geography fosters our knowledge on urban history and the historical impact of federal housing policies by revealing that the heterogeneity of the effects of redlining is closely related to historical land use patterns (Jackson (1980); Greer (2013); Rothstein (2017)).

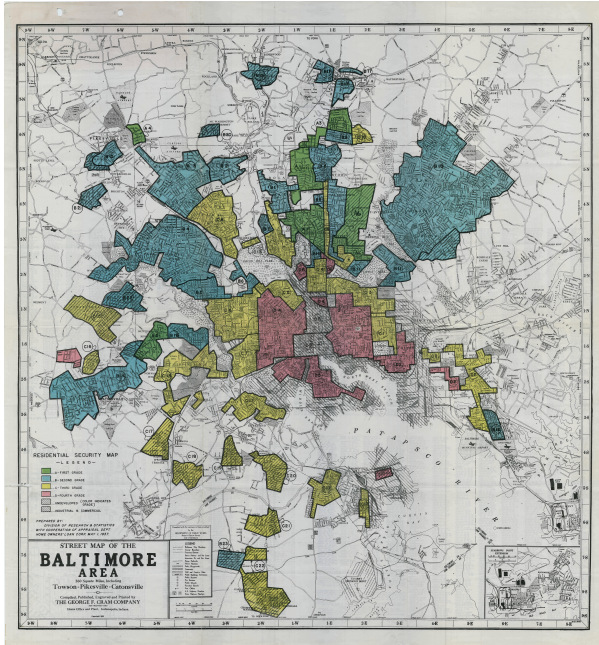
2. Institutional Background

The Great Depression had a significant impact on the housing market, causing housing prices to fall and foreclosures to rise. Nicholas and Scherbina (2013) show that by 1939 the Manhattan real estate market had not recovered from the 1929 crash. Home foreclosures rose from 68,000 in 1926 to 250,000 in 1932 (Jackson, 1987). In 1933, more than 1,000 loans were foreclosed daily and half of the home mortgages were in technical default (Jackson (1987), Wheelock et al. (2008)). Between 1931 and 1935, the foreclosure rate exceeded 1% yearly, and it only returned to 1926 levels by 1941. (Wheelock et al., 2008). Moreover, housing prices declined to the extent that a typical house valued in 5,000\$ in 1926 was only worth 3,300\$ in 1932 (Jackson, 1987). Typical properties in Manhattan bought in 1920 had lost 46% of their initial value 20 years later (Nicholas and Scherbina, 2013).

The administration initiated a series of reforms to stabilize the housing and mortgage markets and assist distressed borrowers. The first attempt, the Federal Home Loan Bank Act, arrived in July 1932 and established a system of Federal banks that ought to be discount banks for home mortgages with a corresponding supervision system (Federal Home Loan Bank Board, FHLBB). However, of the 41,000 homeowners who directly applied for loans during the first

²For instance Pandit, Polyakov, and Sadler (2014), Morales (1980), Netusil, Chattopadhyay, and Kovacs (2010) and Franco and Macdonald (2018) on housing prices; Holtan, Dieterlen, and Sullivan (2015) on social capital, Hoffman, Shandas, and Pendleton (2020) on redlining and urban heat island effects or Kondo, Han, Donovan, and MacDonald (2017) on crime.

Figure 1: HOLC map for Baltimore, 1937



Source: Mapping Inequality, Nelson et al. (2017).

two years of the Act, only three were approved (Jackson, 1987). Effective housing measures started to be implemented after FDR took office in 1933.

The New Deal administration implemented its measures through newly created institutions. The Home Owners' Loan Corporation (HOLC) is the relevant institution for redlining. The HOLC was established in 1933 and started to operate as part of the FHLBB to substitute the inefficient loan provision of the Federal Home Loan Bank Act. Initially, it acted as a "bad bank" issuing bonds to buy mortgages from distressed borrowers and providing them with better conditions, like long-term fully amortized mortgages. Between 1933 and 1935, the HOLC had provided one million such low-interest, self-amortizing, long-term, and uniform payments mortgages. This accounted for over 3\$ billions and mortgages to one-tenth of non-farm owner-occupied housing units or, equivalently, one out of five dwellings receiving HOLC financing (Harriss et al. (1951), Hillier (2003)).

The HOLC active lending program ended in 1935 when the FHLBB established the City Survey Program. Its main task became the introduction of a systematic property appraisal process based on neighborhood characteristics³. The goal was to develop a standardized system to assess the value of the real estate now owned by the Government while ensuring the stability of the mortgage market. The concern leading to the development of the Program was that mortgages could go foreclosed even after refinancing, leaving the Government with assets

³Appraisals were common before the HOLC started to conduct them, the relevance of the HOLC appraisal system was that "*it lay in the creation of a formal and uniform system of appraisal, reduced to writing, structured in defined procedures, and implemented by individuals only after intensive training. The ultimate aim was that one appraiser's judgement of value would have meaning to an investor located somewhere else.*" (Jackson, 1987, p. 197).

whose true value was unknown. In some states, this was a major concern since over 40% of the HOLC refinanced mortgages were foreclosed (Harriss et al., 1951). Between 1935 and 1940, the HOLC evaluated neighborhoods in cities with a population greater than 40,000 inhabitants (239 cities). The appraisal process lead to the creation of the *Residential Security Maps*, commonly known as the redlining maps, due to the ink used to colour the riskiest neighborhoods. As an illustration, Figure 1 shows the redlining map for Baltimore.

The HOLC surveyors worked with local appraisers and lenders to create the redlining maps (Hillier, 2003). The established criteria systematically underrated minority and poor neighborhoods by including the age and housing conditions, transportation, proximity to industries, the socioeconomic condition of the residents, their origin and the racial composition of the neighborhood. Following the FHLBB appraisal manual, neighborhoods were classified into four categories reflecting the desirability of lending in the area. The grades could be A-B-C-D, which were colored green, blue, yellow, and red on the maps. As evidenced by the area description files, the appraisal process reflected the institutionalized racism of the period resulting in the systematical undervaluation of black, immigrant, Jewish, or racially mixed neighborhoods (Jackson (1980), Hillier (2003))⁴. For instance, in the two worst graded areas, there were "*heavy concentrations of low grade aliens*" as in Detroit, or in Staten Island where "*Italian infiltration depress residential desirability in this area*". "*Slow increases of subversive races*" were taking place in Los Angeles and "*coloured infiltration a definitely adverse influence on neighborhood desirability*" in Brooklyn. Areas with a "*community of the best class of Negroes*" as the historical upper-class black communities of Jacksonville were also redlined.

More specifically, according to the FHLBB Appraisal Manual (Hillier, 2005), the grades were described as follows:

- A-graded, greenlined: "Best" neighborhoods were "*homogeneous in demand in good and bad times*".
- B-graded, bluelined: "*Still Desirable*", "*like a 1935 good automobile, but not what people who can afford it are buying today*".
- C-graded, yellowlined: "*Definitely declining*" neighborhoods that were "*suffering from an infiltration of lower grade population*".
- D-graded, redlined: "*Hazardous*" neighborhoods where "*the things that are now taking place in C have already happened*".

According to Jackson (1987), the appraisal process was based on an ecological and socioeconomic theory of neighborhood change. Appraisers believed neighborhood decline was inevitable, due to the increasing age and obsolescence of housing and the consequent filtering towards lower income groups. Simultaneously, the racial composition of the neighborhood determined the housing value⁵. As a result, black and minority neighborhoods would receive

⁴The area description files are available together with the redlining maps on the Mapping Inequality Project of the University of Richmond (Nelson et al., 2017).

⁵The FHA (1936) appraisal manual mentioned that "*the infiltration of inharmonious racial groups [...] tends to lower the levels of land values and to lessen the desirability of residential areas.*" (FHA, 1936, p. 72).

unambiguously the worst grade. Neighborhoods with low rents and aging housing prone to filtering down soon would be in the second worst grade. The best grades were reserved for the newer parts of the city and for areas that could protect from the "*infiltration*" of population groups that represented "*adverse influences*" for housing values stability (Hillier, 2003) through zoning restrictions or private covenants⁶. Thus, worst graded areas were deemed to constitute a lending risk for banks and credit should be restricted⁷.

While it is unclear how publicly available the HOLC maps were and how much they influenced lending decisions, the HOLC is regarded as the primary actor behind redlining due to the diffusion of its standardized appraisal process⁸. The active refinancing program of the HOLC ended in 1936, before the City Survey Program began, suggesting that the maps did not lead the mortgage refinancing (Jackson (1987); Mitchell and Franco (2018)). However, the collaboration of HOLC agents and local brokers contributed to the homogenization of appraisal criteria and implies active lenders followed similar grading techniques.

Until the recent evidence of Fishback et al. (2022), the HOLC lending guidelines were considered the determinants of the ones the FHA followed (Hillier, 2003). The FHA continued providing the long-term fully amortized mortgages the HOLC had discontinued. In fact, the FHA also created its own lending risk maps, although these maps are not available on a large scale⁹. The FHA contributed to the decay of core areas through its predilection towards single-unit rather than multi-unit housing, by offering worse conditions for repair loans, and by virtually only allowing insurance in suburban areas through its lending guidelines and construction standards. By the late 40s, the FHA was providing insurance for one third of the new homes (Aaronson et al., 2021b) and by 1972, the FHA had insured mortgages for eleven million families (Jackson, 1987).

One may never be able to positively assert whether the HOLC maps were publicly used or not. Nonetheless, by reflecting the prevalent appraisal guidelines of America at that period, the HOLC maps serve as an approximation to the discriminatory lending practices of the time. Formally, redlining practices were outlawed when the Community Reinvestment Act (CRA) was passed (1977). The CRA made illegal discriminatory lending on the basis of neighborhood

⁶This has been corroborated by Hillier (2005), Fishback (2014) and Crossney and Bartelt (2005) since they show that both the racial composition and housing characteristics were determinants of the grades in the particular cities they study.

⁷Krimmel (2018) further quotes the instructions given in the manual to local financiers:

Good mortgage lenders are more conservative in the Third grade or C areas and hold loan commitments under the lending ration for the A and B areas. The fourth grade or D areas...are characterized by detrimental influences in a pronounced degree, undesirable population of an infiltration of it... The areas are broader than the so-called slum districts. Some mortgage lenders may refuse to make loans in these neighborhoods and others will lend only on a conservative basis. These maps and descriptions have been carefully checked with competent local real estate brokers and mortgage lenders, and we believe they represent a fair and composite opinion of the best qualified local people.

⁸Researchers like Hillier (2003) and Greer (2013) maintain that the maps were not diffused despite the high demand for them, while others like Jackson (1980) and Woods (2012) defend the opposite.

⁹However, evidence shown in Aaronson et al. (2021b) suggests the FHA grades for Chicago resembled the HOLC ones.

characteristics by establishing that banks should meet the financial needs of the low and moderate-income neighborhoods of the communities they were serving.

3. Data

This paper leverages a new dataset that follows neighborhoods designated by the HOLC surveyors from 1940 to 2015. The digitized HOLC maps define neighborhoods, and a new set of crosswalks matches them with Census data. Geographic data capturing the share of the neighborhood that lies by water features and parks are added to these HOLC neighborhoods. I also develop a new dataset containing all waterfront modifications that have taken place in these cities. Finally, artificial intelligence is used to predict the presence of trees in high-resolution ($1m^2$ pixels) aerial imagery.

The *Mapping Inequality* project of the Digital Scholarship Lab of the University of Richmond has digitized the HOLC maps from the National Archives (Nelson et al., 2017)¹⁰. The result of the digitization is a collection of georeferenced maps that show the location of the neighborhoods drawn by HOLC surveyors, along with the assigned grade (A-B-C-D) and, when available, the area description files surveyors elaborated with the conditions that justified the grade. For estimation purposes, neighborhoods are matched to their corresponding 2010 MSA¹¹. Appendix Table 9.3.6 shows the redlined cities considered, their corresponding 2010 MSA, and the number of neighborhoods with Census data for the 1940-2015 period.

Given that this paper explores the effects of redlining at the neighborhood level, HOLC maps are matched with Census tract (1940-1980) and block-group level data (1990-2015) from the National Historical Geographic System (NHGIS). The analysis is restricted to this period because tract level data is only available from 1930 but limited city coverage. Hence, the analysis starts in 1940 to be able to cover more cities¹². I address the misalignment between Census data and the HOLC maps by constructing data at the HOLC neighborhood maps level with the use of a new set of crosswalks, the Census-to-Redlining Constant Crosswalks. Data at the neighborhood level is the weighted sum of the Census units data that compose the HOLC neighborhood, with weights equal to the areal share of the Census unit that falls within the neighborhood and that was already surveyed as tracts in 1940. To ensure neighborhoods are captured comprehensively since 1940, the procedure imposes the additional restriction that at least 80% of the neighborhood had to be covered by tracts in 1940¹³.

¹⁰At the moment of starting working on this paper (2018-2019), the number of digitized maps was slightly lower. As a result, there are some missing cities that have been added recently to the *Mapping Inequality* project.

¹¹The 2010 definition is used for practical purposes since it is the definition that contains most of graded neighborhoods.

¹²Data availability imposes the additional restriction that I cannot explore the effects of the introduction of redlining and reduces the possibility of exploring pretrends to the set of cities that were surveyed by the census both in 1930 and 1940. Krimmel (2018) performs this comparisons and shows there were no different pretrends between neighbouring D-C areas.

¹³Appendix 9.1 describes in detail how the crosswalks are constructed, provides visual examples and explains how the relevant variables have been constructed.

In contrast to grade assignment procedures followed in the literature to overcome the Census-HOLC misalignment¹⁴, the data construction process preserves the original and sharp variation in assigned grades, ensures a gradual change in the characteristics of adjacent neighborhoods, and eliminates the measurement error caused by grade assignments. Hence, these crosswalks meet the requirements of the empirical strategy to estimate the effects of redlining. The only concern of using these crosswalks would arise if a very heterogeneous tract is split into different grades or if a graded neighborhood is composed of heterogeneous tracts. By the design of the data sources, this is a minor concern since Census units are designed to be homogeneous areas, and graded neighborhoods were deemed to represent fairly homogeneous areas by HOLC surveyors¹⁵.

Next, I use data for water and parks as natural amenities. The choice is motivated by the evidence showing their relevance for neighborhood outcomes and by the fact they are the amenities with enough variation among nearby areas (Jackson (1987), Brueckner, Thisse, and Zenou (1999), Rappaport and Sachs (2003), Lee and Lin (2018), or the survey on the impact of parks by Crompton and Nicholls (2019)). Data on water features is collected from the Coastal Geospatial Data project of the National Oceanic Atmospheric Administration (NOAA) and includes the shoreline, Great Lakes, any other lake, and major rivers. For parks, the data relies on the ESRI layer on parks provided by the UCLA geoportal. To capture meaningful natural amenities, data for lakes and parks is restricted to the set of lakes named "lake" or "pond" and to parks named "parks", "gardens", or "forests".

A neighborhood is defined as *having* water and parks natural amenities when at least 20% of its area is covered by a 500-meter buffer around any of the features¹⁶. The area threshold was determined by visual inspection of the neighborhoods that would be defined as having such amenities under different thresholds. Low thresholds do not capture meaningful situations whereas excessively high thresholds select very specific neighborhoods. The 20% criterion balances both, in the sense that it is restrictive enough to capture meaningful natural amenities and differences among adjacent neighborhoods but not enough to lead to concerns on sample selection.

Also, I hand collect and geolocate data on waterfront modifications in the cities under study. This dataset was created using data from a variety of sources including departments of parks, local history and news, tourism offices, and redevelopment and planning agencies. In most cases, the redevelopment plans resulted in the creation of parks, greenways, or promenades that can be easily geolocated. In other cases, the districts where the project was implemented or

¹⁴As in Hillier (2005); Appel and Nickerson (2016) Krimmel (2018) among others.

¹⁵There is evidence in the area descriptions that there was heterogeneity within neighborhoods, however entropy indices (not shown) in both in 1940 and 2015 were on average around zero, meaning that the Census units in neighborhoods have essentially a very similar composition in terms of population, home values and family income.

¹⁶The reason to use areas and not distances is because graded neighborhoods tend to have irregular shapes and thus centroids, being means of vertices, are not guaranteed to fall inside and would not allow to capture the real presence of amenities in the neighborhood.

the coordinates of the created place are used as geolocation¹⁷. Neighborhoods are considered as having a modified waterfront when they intersect a 500-meter buffer around a geolocated modification. Appendix Table 9.3.8 contains the list of modifications intersecting neighborhoods. A detailed description of the data is available in Appendix 9.2.

Typically, research exploring the role of trees has relied on tree surveys with coverage restricted to particular cities and, in very few cases, more than one year. Moreover, recent machine learning algorithms require training data whose availability at high-resolution and large scales is a recent phenomenon (near-infrared light, NIR) or, due to its costs, its geographic and time availability is restricted (Lidar). To overcome this limitation, I propose a new method to train data from older periods with recent NIR data and produce the first panel of tree coverage in more than 30 US cities.

This paper implements the pixel classification algorithms developed by Yang et al. (2009) and Bosch (2020) on the National Agricultural Imagery Product (NAIP) to construct data on tree canopy. The NAIP is a program developed by the US Department of Agriculture since 2003. Its main goal is to acquire and publish high-resolution ($1m^2$ or less) aerial images taken during the agricultural growing season and is reconducted every 3 years since 2009. The images contain, for every $1m^2$ pixel, the red-green-blue (RGB) channels of the underlying color and, for recent years, also the non-visible NIR band. Due to the time cost of predicting tree canopy, only two periods are considered trying to maximize the time difference to guarantee observing changes in tree canopy. Given that the first available year differs across states, the first period ranges between 2003/2007 and the second one between 2014/2015. Appendix Table 9.3.7 shows the periods for every city considered.

In contrast to most tree detection algorithms that are intensive in data requirements, Yang et al. (2009)'s method has the advantage of achieving similarly good results using only RGB data. The accuracy of the prediction relies on training the algorithm with precise ground-truth masks. The masks are usually produced using limitedly available NIR or Lidar data. To overcome this limitation, I employ various visual graphic techniques to automatically train the data of the first period with the recent NIR data¹⁸. Given that Yang et al. (2009)'s algorithm relies exclusively on RGB colors, potential inaccuracies could appear if the colors of training data of the second period differ from the ones of the test data (i.e., lighting conditions may change hues). I avoid this concern by equalizing the lightness and color histogram of all first-period

¹⁷These modifications are restricted to those that were direct attempts by cities, which means that waterfronts that might have revitalized from the unplanned action of individuals by setting commercial or leisure venues are not considered.

¹⁸This non-visible light captures alive vegetation since the photosynthesis is a light absorption-reflection process whereby alive vegetation absorbs the visible red light generating heat and reflects the NIR light to keep a stable temperature.

images to their counterpart in the second period as a pre-step¹⁹. Appendix Figure 9.3.5 shows an example of the color histogram equalization process. To find the tree pixels in the training images, I first compute the widespread used normalized difference vegetation index (NDVI) as $\frac{NIR-R}{NIR+R}$. This index ranges from -1 to 1, with higher values representing the densest and most alive vegetation. Because the particular values that differentiate trees depend on lighting conditions, soil characteristics, crop type, and growing stage of the tree, image thresholding is applied to obtain a separating value for each particular training tile. The threshold is determined by finding the two values that maximize the variance between three pixel classes and minimize the within-class variance (i.e., Otsu's thresholding). Since most urban areas exhibit mixed features characterized by different NDVIs, double segmentation guarantees the highest threshold captures the class that has the most alive (i.e., higher chlorophyll content) and dense vegetation, which corresponds to trees²⁰. Appendix Figures 9.3.3 and 9.3.4 illustrate the functioning of the thresholding algorithm. Examples of the predictions generated by the algorithm are shown in Appendix Figures 9.3.1 and 9.3.2²¹.

I construct the change in exposure to plagues by merging the data on county presence of plagues as of December 2015 compiled by Fei et al. (2019) and hosts potential distribution of Wilson, Lister, Riemann, and Griffith (2013). The data on the first detection from Fei et al. (2019) is supplemented with data from multiple sources to obtain the most accurate detection date possible. In the best cases, it is obtained at the city level from cities or states information on a particular plague. In other cases, it is information at the state level. Fei et al. (2019) also provide the list of potential host species for each plague, which is merged with the estimated tree species distribution by Wilson et al. (2013). The species distribution is represented as a raster for each tree species, in which each $250 \times 250m$ pixel represents the predicted live-tree basal area of that species using reference data between 2000-2009. Of the total 162 potential host species of the plagues, Wilson et al. (2013) provide the species distribution of 130 of them. I create a new raster for each plague by adding the basal areas of all of its potential hosts and then obtain the total basal area for each neighborhood. Potential host exposure in a neighborhood is computed as the ratio of total basal area to detected trees in 2000. Appendix Figures 9.3.6 and 9.3.7 show

¹⁹In practice, histogram equalization is applied on the CIE $L^*a^*b^*$ color space. The reason to use this color space is that in the RGB color space, each channel (red-green-blue) has information on, not only “color”, but also hue, saturation, chroma, and lightness. Since joint-histogram matching proved too time-consuming, matching each RGB channel independently yielded images where colors would differ considerably from the second-period ones. After comparing histogram matching with different color spaces where “colors” were a separated channel (i.e., HSV, LCH, etc.), CIE $L^*a^*b^*$ was the one that led to better equalization, since it matches separately lightness (L^*), red-green (a^*), blue-yellow (b^*). Once the three channels are matched, the image is reconverted to RGB so that the algorithm can be implemented.

²⁰As pre-processing steps, the NIR band is, first, smoothed with Gaussian filters. A first single-level Otsu's thresholding is used to eliminate pixels the lowest part capturing shadows and some man-made surfaces. This allows to smooth the NDVI distribution and reduce false positives. To remove noise and increase the accuracy of the thresholds, NDVI distribution is also smoothed by applying a Gaussian filter to the NDVI before implementing the two-level Otsu's thresholding. Additionally, since some areas may only capture water surfaces, whenever a tile has only negative NDVI values (i.e., there are only water surfaces), all pixels are automatically set to not-tree.

²¹For further details, see the original paper by Yang et al. (2009) and the implementation developed by Bosch (2020).

the county distribution of the total number of plagues as well as the distribution of potential hosts respectively.

Lastly, I obtain data from the Opportunity Atlas (Chetty, Friedman, Hendren, Jones, and Porter, 2018) to provide insight into the drivers of the estimated effects²². The Opportunity Atlas provides adulthood socioeconomic and mobility variables by parental income, gender, and race for children born in a particular Census Tract between 1978 and 1983, just after the outlawing of redlining. The analysis will focus on outcomes related to geographic and intergenerational mobility, since considering these variables potentially allows to differentiate neighborhood development from gentrification. Since the data is available at the tract level, I create a specific crosswalk for 2010 tracts with the same procedure used for the Census-to-Redlining Constant Crosswalks.

The sample consists of 3,684 graded neighborhoods per decade, with approximately 60% having natural amenities. In terms of population, the data accounts for nearly 20% of the total US population in 1940. However, the population is not evenly distributed among categories and is heavily concentrated in D and C neighborhoods: despite accounting for 66% of graded neighborhoods, D and C areas together contain over 80% of the sample population. There are also racial disparities in population distribution: 97% of the black population in the sample is concentrated in D and C areas, while only 3% is found in the best two categories. This population distribution corroborates the fact that redlining mainly affected black communities²³.

This paper focuses on the evolution of the white population share, home values, and family income because as discussed in Section 2 they determined the assigned grade, these variables are more likely to have been influenced by redlining and there is evidence that natural amenities influence them (Villarreal (2014), Lee and Lin (2018), Heblitch et al. (2021))²⁴. Regarding race, the racial component behind redlining was already discussed in Section 2²⁵. Next, I focus on home values measured as the percentage of owner-occupied housing units that are on and above the

²²Although this exercise is similar in spirit to Aaronson, Faber, Hartley, Mazumder, and Sharkey (2021a)'s analysis of the causal effects of redlining in intergenerational mobility, the aim is to use the Opportunity Atlas as an approximation of the changes that accompany the heterogenous D-C convergence.

²³See Appendix Tables 9.3.1 and 9.3.2.

²⁴The reason to exclude other variables that could have been relevant is that there is no clear intuition regarding how natural amenities will affect them. For instance, as much as changes in housing units can capture the effect on real state industry of redlining policies (Krimmel, 2018), it may also be the case that areas with natural amenities have lower housing units because of zoning restrictions or the presence of commerce and services. Educational attainment and unemployment will also be linked to job's location and commuting patterns.

²⁵I follow only white population because the share of population from other races affected by redlining, besides white and black population, is very low and concentrated in particular areas. Thus, the key differences in terms of population are between black and white population and therefore, in terms of shares, it is enough to focus on one of them alone.

Table 1: neighborhood change: 1950-2015

Panel A: Share below in 1950			
	White population	Home Values	Income
A-Green	0.45	0.05	0.22
B-Blue	0.36	0.21	0.28
C-Yellow	0.43	0.55	0.51
D-Red	0.74	0.85	0.80
Panel B: Share still below in 2015			
	White population	Home Values	Income
A-Green	0.21	0.58	0.10
B-Blue	0.38	0.58	0.34
C-Yellow	0.59	0.69	0.64
D-Red	0.70	0.66	0.71

Notes: Table shows the share of neighborhoods of each grade that were below the MSA medians in 1950 (Panel (A)) and the share of those that was still below in 2015 (Panel B).

Source: see data description. Own elaboration.

MSA median home values²⁶. Because housing accounts for a large portion of household wealth, the persistent wealth gap between black and white populations may be related to the impact of redlining on segregation and depressed home values. Finally, family income is measured as the percentage of families that are on and above the MSA median family income²⁷.

4. The persistence of redlining

The primary identification challenge to estimating the persistence of redlining stems from the design of the HOLC grading process. As discussed in Section 2, the assigned level of credit restrictions reflected housing and demographic characteristics of neighborhoods by the late 30s. Hence, the absence of random assignment to treatment implies causality cannot be directly inferred using a traditional differencing strategy because neighborhoods were already different when credit restrictions were introduced. Appendix Tables 9.3.3 and 9.3.4 show the discontinuities in population, housing values and income for each grade in 1940 and how they have persisted in 2015.

Table 1 provides additional evidence on neighborhood transition and grade discontinuities from 1950 to 2015. Panel A shows the share of neighborhoods of each grade that were below the MSA median in terms of the share of white population, home values, and family income in 1950,

²⁶The MSA medians are computed, for every decade, with the tracts/block groups whose centroids fall in the MSA. Hence, every decade new areas are added to the MSA since restricting the comparison to the HOLC map area could have lead to overestimating effects by neglecting newly developed areas that could be exercising an upward pressure at the MSA level. Given that these variables are reported by bins, I assign the midpoint to each bin or keep the value for the lowest and higher bin. I then obtain the medians with this midpoints, using as weights the number of housing units/families of each bin.

²⁷Family income is defined as family income in the previous year. It is only available since 1950.

reflecting discontinuities were also relative to the MSA: D areas have the greatest proportion of neighborhoods that are below the MSA medians^{28,29}. Panel B of Table 1 provides insight into the persistence of neighborhood trajectories by displaying the share of neighborhoods that are still below the MSA medians in 2015. The trajectories of neighborhoods persist over time: most of the neighborhoods below MSA medians in 1950 are still below in 2015. Moreover, persistence varies by grade and is strongest in D neighborhoods. Adding the evidence from the two panels suggests that most D areas remained behind in 2015.

Overcoming the identification challenges caused by the HOLC grading process requires comparing similar areas that faced different levels of credit restrictions. Motivated by the HOLC grades, only C-graded areas constitute the control group since they were the areas considered more similar to D ones and to be in the previous step before converging to a D zone. Evidence in Table 9.3.2 provides additional supporting evidence since it shows that the D and C areas have the smallest differences in neighborhoods in 1940. The D-C comparison has the additional advantage of capturing a discrete jump in the credit policy: from complete credit restriction (D) to conservative lending (C) as mentioned by Krimmel (2018).

The D-C comparison is performed at two different levels. The first level restricts the analysis to areas within the same MSA³⁰. Adding MSA fixed effects to the diff-in-diff equations controls for MSA unobserved and time-invariant characteristics. The second one imposes further restrictions since, even within an MSA, areas may evolve in different ways subject to other unobserved factors. To overcome this concern, this paper follows the usual approach in redlining literature and restricts the analysis to adjacent C-D areas that share the longest borders, similar to Aaronson et al. (2021b) and Krimmel (2018)³¹. C-D bordering areas represent sudden changes in grades but, being adjacent areas, they share the same unobservable and local characteristics, and thus, the grade assignment is *as good as random*³². The procedure resembles regression discontinuities usually employed in the education economics literature that exploit falling a different sides of a grade cut-off³³. In the redlining setup, there is a similar grade cut-off between receiving the worst credit rating (D) and the second worst (C), and the threshold from the cut-off is defined geographically by being adjacent and sharing the

²⁸In this table the MSA median is computed only by looking at the HOLC map areas that fall in the MSA (2010 definition). Thus, this is not the same normalization as the one done for home values and income.

²⁹The share of green neighborhoods below the MSA median in terms of white population is virtually the same as for the yellow ones. The fact that green areas were not very populated is a potential explanation. In 1950 (not shown), only around 4% of the sample population was located in these areas.

³⁰The term *city* is used to reference the maps designation of cities. These surveyors' definitions of *cities* are cumbersome since they tend to divide areas in different maps (i.e., the 5 boroughs of New York). Hence, HOLC neighborhoods are matched to the corresponding MSA (2010 definition) to avoid these situations.

³¹The choice of neighboring areas on the basis of border length is made in this paper because, given the irregular shapes of HOLC neighborhoods, using centroids or coordinates as Krimmel (2018) does not allow to make a meaningful restriction.

³²Appel and Nickerson (2016) follow a similar approach but comparing D areas to any other graded adjacent area. This strategy is unlikely to correct non-random grade assignments since the areas compared are very different and were also subject to different lending policies.

³³See for instance Ost, Pan, and Webber (2018).

longest borders, in a similar fashion as in border regression discontinuity. Adding border-pair fixed effects guarantees any common and time-invariant unobservable factor for the pair of neighborhoods is controlled for³⁴.

One requirement for the empirical design to isolate the effect of redlining is that there is a sharp variation in the assigned grade at the border, but neighborhood characteristics change gradually. As a result, guided by this requirement, data is constructed at the originally graded neighborhood level to preserve the original sharp variation in grades, but by assigning Census units to graded neighborhoods, unobservable neighborhood characteristics change gradually at the border.

Formally, the goal is to estimate the persistence of redlining using a diff-in-diff with two dimensions, redlining and the passing of the CRA. Let y_{imt} be the relevant dependent variable in HOLC neighborhood i at MSA m in year t , R_i be the redlining grade (1 if D, 0 if C) and $Post^{1977}$ represent the passing of the CRA (1 from 1980 onward, 0 until 1970), then the overall persistence of redlining can be estimated with the following equation:

$$y_{imt} = \beta_0 + \beta_1 R_i + \beta_2 (R_i \times Post^{1977}) + \alpha_{im} + \gamma_t + \epsilon_{imt} \quad (1)$$

where α_{im} represents either MSA fixed effect or border-pair fixed effects, γ_t are year fixed effects and ϵ_{imt} is the error term³⁵. In this regression, the coefficient of interest would be β_3 since it would reflect the catching up after between D and C areas after the outlawing of redlining.

The estimates of Equation 1 at the within MSA and border-pair are shown in Table 2 and Table 3 respectively. Both tables lead to the same conclusions. Focusing on the first row, the coefficient for being D-graded is negative and statistically significant: $\beta_1 < 0$ in Equation 1. This shows that, during the years of redlining (1950-1970), there were negative significant gaps for D areas, compared to their C neighbors. The coefficient of the interaction between D-grade and the passing of the CRA is, however, positive and strongly significant: $\beta_2 > 0$ in Equation 1. This coefficient indicates that, after the removal of redlining, there is some degree of convergence for all the variables. However, adding up the two coefficients (i.e., $\beta_1 + \beta_3$ in Equation 1) shows that the D-C gaps are still present after the removal of redlining. Hence, the effects of redlining do not disappear and are persistent over time.

Given that the estimates of the within MSA comparison can be biased in the presence of local unobserved factors, I provide a quantification of the border-pair results in Table 3. During

³⁴Aaronson et al. (2021b) follow a more strict design and construct small buffers at each side of the C-D border. However, following such a procedure would not allow me to incorporate geography in the analysis, since it is unlikely to find differences in geography at small distances.

³⁵Note that, in my specifications with border-pair fixed effects, MSA fixed will be fully absorbed by the border-pair ones. Moreover, since year fixed effects are introduced, the variable $Post^{1977}$ would be collinear to these fixed effects. Given the data construction process, the number of observations per decade and MSA is relatively low and hence MSA-year fixed effects to control for time-trends cannot be included since there is not enough variation to estimate them. For the same reason, standard errors cannot be clustered at the MSA-decade level since clustering requires having enough observations per cluster. As a result, the standard errors provided will be simple robust standard errors.

Table 2: Persistence of redlining, within MSA

VARIABLES	(1)	(2)	(3)
	White Share	% HU above MSA MHV	% Families above MSA MFI
D-graded	-0.144*** (0.00635)	-0.179*** (0.00588)	-0.112*** (0.00349)
D-graded \times Post ¹⁹⁷⁷	0.0547*** (0.00839)	0.0948*** (0.00761)	0.0327*** (0.00475)
Observations	19,460	19,418	19,454
Year FE	YES	YES	YES
MSA FE	YES	YES	YES
Border-pair FE	NO	NO	NO
Sample	All D-C	All D-C	All D-C
Adjusted Within R-squared	0.0354	0.0537	0.0709
Mean Dep. Var	0.635	0.409	0.429

Robust standard errors in parentheses

*** p<0.01, ** p<0.05, * p<0.1

Notes: This table shows the results of estimating Equation 1 using the entire D-C sample. The Post¹⁹⁷⁷ period is 1980-2015. All variables are described as in the text. HU stands for housing units, MHV for median house vale and MFI for median family income.

Table 3: Persistence of redlining, within D-C pair

VARIABLES	(1)	(2)	(3)
	White Share	% HU above MSA MHV	% Families above MSA MFI
D-graded	-0.0847*** (0.00670)	-0.0946*** (0.00638)	-0.0593*** (0.00373)
D-graded \times Post ¹⁹⁷⁷	0.0435*** (0.00777)	0.0578*** (0.00754)	0.0185*** (0.00463)
Observations	9,632	9,629	9,632
Year FE	YES	YES	YES
MSA FE	Absorbed	Absorbed	Absorbed
Border-pair FE	YES	YES	YES
Sample	Bordering D-C	Bordering D-C	Bordering D-C
Adjusted Within R-squared	0.0324	0.0371	0.0506
Mean Dep. Var	0.592	0.344	0.390

Robust standard errors in parentheses

*** p<0.01, ** p<0.05, * p<0.1

Notes: This table shows the results of estimating Equation 1 using the bordering D-C sample. The Post¹⁹⁷⁷ period is 1980-2015. All variables are described as in the text. HU stands for housing units, MHV for median house vale and MFI for median family income.

the years of redlining the share of white population would be 8 percentage points lower in D neighborhoods, compared to their C pairs; relative to their C counterparts, D areas would have 9 percentage points lower shares of housing units on and above the MSA median home value and 5 percentage points lower shares of families on and above the MSA median family income. After the passing of the CRA, the gap between white population would be around 50% of the previous gap, around 40% in home values, and about 70% for family income³⁶.

To discern the timing pattern behind the effects, I modify Equation 1 by letting the *Post*¹⁹⁷⁷ dummy take value zero for the redlining year (1950-1970) and a different value for each decade afterwards³⁷. The interaction between D-grade and the new post variable will show the yearly change in the gap, relative to the years when redlining was legal. The estimated coefficients of this interaction for each variable, together with the 95% confidence intervals, are shown in Figure 2.

The results show that the effects of removing redlining occur as soon as it is prohibited, because the 1980 coefficient is positive and statistically significant for all variables³⁸. This implies that the partial convergence is driven by redlining removal rather than recent neighborhood events. The patterns depicted in Figure 2 indicate convergence occurs gradually and spreads over time³⁹. Despite convergence, the effects do not vanish entirely during the period, implying interventions are needed since removing the credit restriction is insufficient to allow neighborhoods to develop.

5. The heterogeneous persistence of redlining and natural amenities

The findings in Section 4 are consistent with redlining literature because they show that redlining has long-lasting effects. This literature, however, has not attempted to explore the heterogeneity of these effects or their causes. Overlooking the heterogeneous persistence of redlining makes it difficult to conclude that discriminatory lending practices still affect neighborhoods, because this persistence may occur only in certain areas or under certain conditions.

In this section, I link the heterogeneity of the effects to the presence of water and parks natural amenities, motivated by the literature showing they are key determinants of neighborhood long-run trajectories and can explain the persistent differences among neighborhoods. The underlying hypothesis is that the long-run effects of redlining have been heterogeneous and less

³⁶This is computed by adding up the two coefficients and dividing them by the redlining one.

³⁷Instead of including year fixed effects, this variation adds the newly defined dummy *Post*¹⁹⁷⁷, which is virtually the same as the fixed effects

³⁸Additional supporting evidence for this can be found in Appendix Tables 9.3.9 and 9.3.10, where Equation 1 is estimated restricting the *Post*¹⁹⁷⁷ to 1980

³⁹For income, there is no such a clear time trend. However, this is not necessarily wrong and would be consistent with neighborhood change and household sorting. The passing of the CRA could be leading to faster effects in terms of population and values and, as these effects take place, they will affect the income of the families that decide to move to a neighborhood.

Figure 2: Timing of the effects

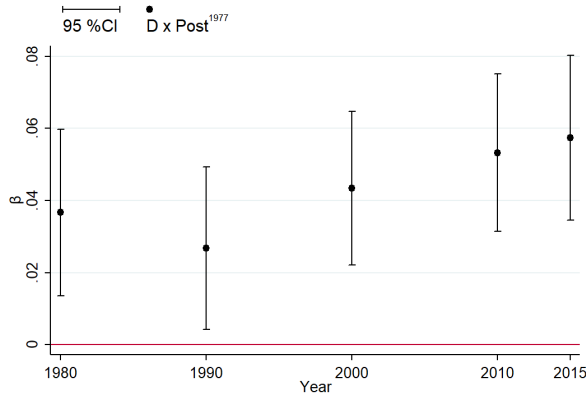


Figure A: White Share

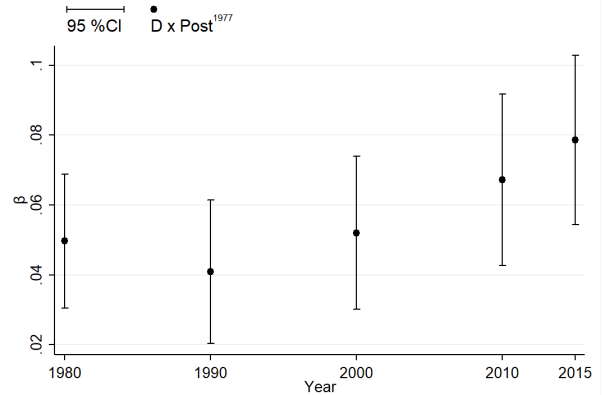


Figure B: Home Values

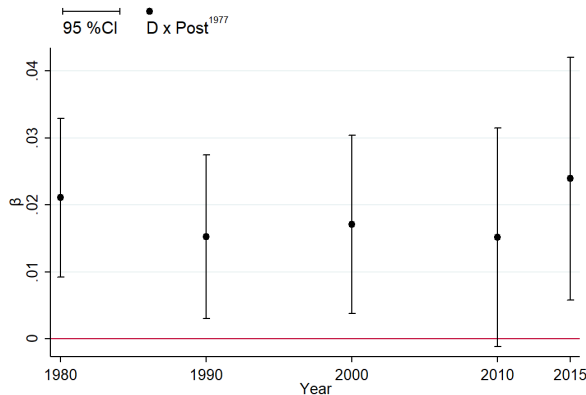


Figure C: Family Income

Notes: Figure shows the coefficient β_3 of estimating: $y_{imt} = \beta_0 + \beta_1 R_i + \beta_2 Post^{1977} + \beta_3(R_i \times Post^{1977}) + \alpha_{ij} + \epsilon_{imt}$, where $Post^{1977}$ takes values zero between 1950-1970 and a different value for each decade after the removal of redlining. Estimated on the adjacent subsample. Dependent variable in Figure A is the share of white population; percentage of housing units on and above the MSA median home value in Figure B; percentage of families on and above the MSA median family income in Figure C.

Table 4: Redlining and natural amenities, within MSA

VARIABLES	(1) White Share	(2) % HU above MSA MHV	(3) % Families above MSA MFI
D-graded	-0.133*** (0.0104)	-0.135*** (0.00977)	-0.0945*** (0.00576)
Natural Amenities	0.0233*** (0.00670)	0.0242*** (0.00782)	0.00860** (0.00402)
D-graded × Natural Amenities	-0.0189 (0.0131)	-0.0711*** (0.0122)	-0.0286*** (0.00722)
D-graded × Post ¹⁹⁷⁷	0.0589*** (0.0138)	0.0706*** (0.0125)	0.0268*** (0.00772)
Natural Amenities × Post ¹⁹⁷⁷	0.0357*** (0.00986)	0.0214** (0.0101)	0.0189*** (0.00567)
D-graded × Natural Amenities × Post ¹⁹⁷⁷	-0.00901 (0.0174)	0.0368** (0.0157)	0.00816 (0.00979)
Observations	19,460	19,418	19,454
Year FE	YES	YES	YES
MSA FE	YES	YES	YES
Border-pair FE	NO	NO	NO
Sample	All D-C	All D-C	All D-C
Adjusted Within R-squared	0.0399	0.0577	0.0738
Mean Dep. Var	0.635	0.409	0.429

Robust standard errors in parentheses

*** p<0.01, ** p<0.05, * p<0.1

Notes: This table shows the results of estimating Equation 2 in the entire D-C sample. The Post¹⁹⁷⁷ period is from 1980-2015 and the redlining period from 1950-1970. HU: Housing Units. MHV: Median Home Value. MFI: Median Family Income. Natural amenities is a dummy variable that takes value one for those neighborhoods in which the 500m buffers around water features or parks cover at least 20% of the area.

persistent in areas that lay by natural amenities. This relationship is modeled by introducing an additional dimension representing natural amenities (A_i) in Equation 1:

$$y_{imt} = \beta_0 + \beta_1 R_i + \beta_2 A_i + \beta_3 (R_i \times A_i) + \beta_4 (R_i \times Post^{1977}) + \beta_5 (A_i \times Post^{1977}) + \beta_6 (R_i \times Post^{1977} \times A_i) + \alpha_{im} + \gamma_t + \epsilon_{imt} \quad (2)$$

where all variables are defined as in Equation 1. The main coefficient of interest is β_6 since it will capture if the catching-up is faster for D areas with water and parks natural amenities.

Table 4 and Table 5 show the results of estimating Equation 2 at the MSA and bordering level, respectively. Focusing on the second and third rows of both tables reveals the impact of natural amenities during the years of redlining. For D areas, it is always the case that natural amenities lead to greater D-C gaps since the coefficients are always negative and statistically significant for home values and housing units. At the border-pair level, this would also be the case for C areas. These negative signs do not necessarily challenge the hypothesis that amenities have a

Table 5: Redlining and natural amenities, within pair

VARIABLES	(1) White Share	(2) % HU above MSA MHV	(3) % Families above MSA MFI
D-graded	-0.0781*** (0.0113)	-0.0761*** (0.0106)	-0.0512*** (0.00575)
Natural Amenities	-0.00967 (0.0115)	-0.0186* (0.0107)	-0.0128** (0.00632)
D-graded × Natural Amenities	-0.0110 (0.0145)	-0.0309** (0.0138)	-0.0136* (0.00794)
D-graded × Post ¹⁹⁷⁷	0.0270** (0.0125)	0.0399*** (0.0120)	0.0140** (0.00689)
Natural Amenities × Post ¹⁹⁷⁷	0.0170 (0.0114)	0.0333*** (0.0106)	0.0248*** (0.00633)
D-graded × Natural Amenities × Post ¹⁹⁷⁷	0.0274* (0.0160)	0.0297* (0.0154)	0.00761 (0.00924)
Observations	9,632	9,629	9,632
Year FE	YES	YES	YES
MSA FE	Absorbed	Absorbed	Absorbed
Border-pair FE	YES	YES	YES
Sample	Bordering D-C	Bordering D-C	Bordering D-C
Adjusted Within R-squared	0.0343	0.0420	0.0545
Mean Dep. Var	0.592	0.344	0.390

Robust standard errors in parentheses

*** p<0.01, ** p<0.05, * p<0.1

Notes: This table shows the results of estimating Equation 2 in the bordering D-C sample. The Post¹⁹⁷⁷ period is from 1980-2015 and the redlining period from 1950-1970. HU: Housing Units. MHV: Median Home Value. MFI: Median Family Income. Natural amenities is a dummy variable that takes value one for those neighborhoods in which the 500m buffers around water features or parks cover at least 20% of the area.

positive impact on neighborhood trajectories. The impact of amenities on neighborhoods can change over time as preferences for amenities and, as will be discussed later, their use change. Given that amenities have a positive effect on C neighborhoods within the MSA, it is possible that at the border-pair, spillovers from D areas with natural amenities have a negative effect on their C counterparts.

Focusing on the interaction of redlining, natural amenities, and the passing of the CRA, amenities have an unambiguously positive effect and imply that convergence in population and housing values is stronger for areas with natural amenities⁴⁰. As in the previous section, the results show similar D-C gaps during the years of redlining for areas with no amenities and that these areas also experiment with a similar degree of convergence, with the minor difference that the new estimates are relatively smaller because they capture differences for areas with no amenities rather than overall differences as in Tables 2 and 3.

The degree of persistence of D areas with no natural amenities is determined by adding the coefficient of D grades and the one of interaction between the grade and the passing of the CRA ($\beta_1 + \beta_4$ in Equation 2). In D areas, the share of white population would still be around 5pp lower, the share of housing units with home values above the MSA median value would be approximately 3pp lower and the share of families above the MSA median family income would be around 4pp lower also. After the CRA, D areas with amenities ($\beta_1 + \beta_3 + \beta_4 + \beta_6$) would still have a 3 pp lower share of white population, 3 pp lower share of housing units on and above the MSA median value, and a 1 pp lower share of families on and above the MSA median income. These gaps translate to a reduction in the previous difference of 60% for white population, 66% for home values, and 34 % for family income, decreases that are much higher than for areas with no amenities (35% for population, 53 % for home values and 28 % for income)⁴¹. As a result, this finding lends support to the hypothesis that the persistence of redlining is heterogeneous, and that natural amenities not only contribute to heterogeneity but also allow for greater convergence.

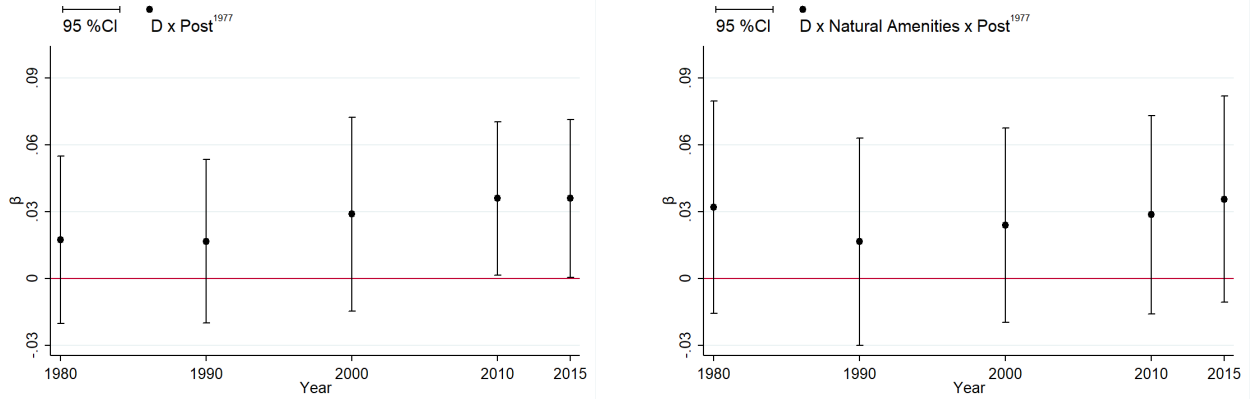
As in Section 4, I re-estimate Equation 2 using the bordering strategy and substituting the dummy *Post*¹⁹⁷⁷ for a dummy that takes value zero during the redlining years (1950-1970) and a different value for the years after. Figure 3 shows the coefficients for each year and 95% confidence intervals. A moderate gradual-accumulating pattern only holds for home values and population in D areas with no amenities, and convergence has stagnated in recent years. For family income, convergence in areas without amenities is sudden and stagnant. For D

⁴⁰At the border-pair, I find that convergence would be stronger in these areas both for the share of white population and home values. Not finding a significant effect on income can be simply related to the fact that neighborhood change is a medium-long run phenomenon and household sorting depending on income takes place on a longer period, when the share of white population and home values have already changed. Within MSA, I only find stronger and more significant convergence in home values. No longer finding the effect for the white share relates to the fact that redlined cities were cities with high share of the black population and they also experimented with an increased inflow of black population (Aaronson et al., 2021b). Hence, it is possible to find no convergence within an MSA but convergence at the border-pair.

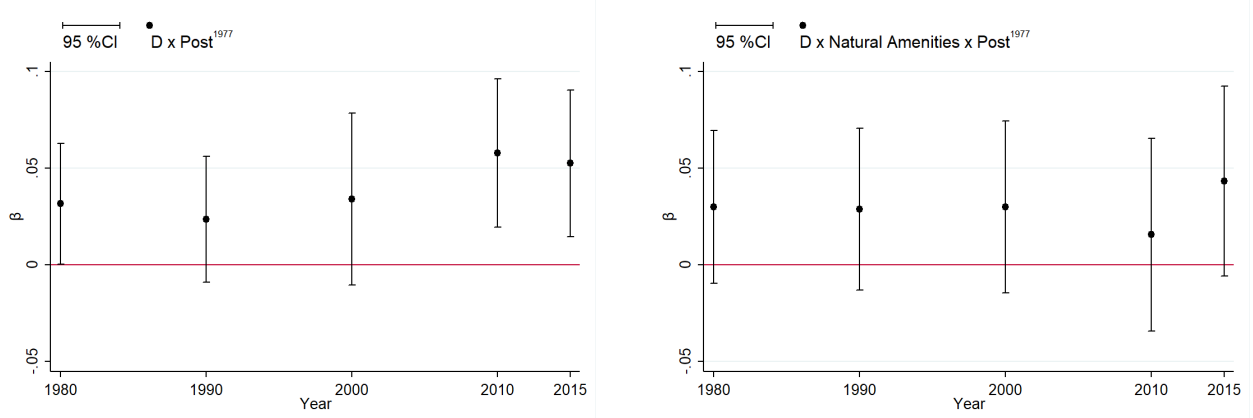
⁴¹The decrease is computed as one minus the ratio of the new gap to the previous gap. For areas with amenities, this ratio is then $\frac{\beta_1 + \beta_3 + \beta_4 + \beta_6}{\beta_1 + \beta_3}$ and for areas with no amenities it is given by $\frac{\beta_1 + \beta_4}{\beta_1}$.

Figure 3: Natural amenities and timing of the effects

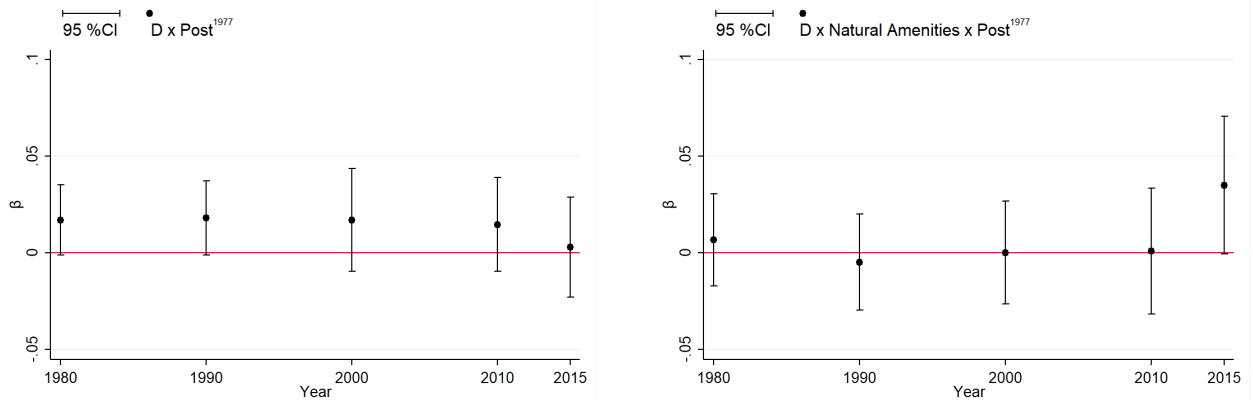
Panel A: White Population



Panel B: Home Values



Panel C: Family Income



Notes: Figure shows the coefficient and 95 % confidence intervals of β_5 and β_7 of estimating on the bordering subsample: $y_{int} = \beta_0 + \beta_1 R_i + \beta_2 A_i + \beta_3(R_i \times A_i) + \beta_4 Post^{1977} + \beta_5(R_i \times Post^{1977}) + \beta_6(A_i \times Post^{1977}) + \beta_7(R_i \times A_i \times Post^{1977}) + \alpha_{ij} + \epsilon_{int}$, where $Post^{1977}$ takes values zero between 1950-1970 and a different value for each decade after the removal of redlining.

areas with natural amenities, the catch-up starts in recent years. The implication is that the gradual-accumulating convergence of Figure 2 emerges from the combination of two effects: the gradual change for areas with no amenities and the recent change for neighborhoods with amenities. Therefore, it invalidates the hypothesis that effects will fade over time and highlights the importance of understanding the heterogeneity of redlining effects.

Robustness

To assess the robustness of the results, I perform a series of tests shown in the Appendix. First, I use the bordering D-C strategy to perform a placebo test and re-estimate Equation 2 with placebo grades. Appendix Table 9.3.11 shows the results. None of the placebo D grade coefficients are statistically significant. Significant effects are only found for natural amenities, which would have a positive and statistically significant effect after the passing of the CRA and a negative one during the redlining years, as discussed previously. This finding supports the hypothesis that natural amenities are important determinants of neighborhood trajectories.

The 20% threshold was chosen to balance capturing meaningful natural amenities and not falling in a selected sample. Changing the threshold to conduct robustness tests would capture different situations rather than providing supporting evidence on the impact of natural amenities. Thus, rather than using different thresholds, I use a different definition for natural amenities that has the same essence as the 20% threshold. Natural amenities are defined as the situation in which the share of a neighborhood covered by any water feature or park is strictly greater than the MSA median, weighted by neighborhood area. This definition allows capturing both meaningful natural amenities, since they are above the median for the MSA, and, at the same time, not having an extremely selected sample since it will consider, for MSAs that have any of the natural amenities, all areas above the median. Results from estimating Equation 2 are shown in Appendix Table 9.3.14. The results are robust to using both definitions. The only relevant change would be the absence of a significant interaction between D-natural amenities and post-CRA in the share of white population. However, the results for white population in Table 2 are mainly driven by recent years (see Panel A of Figure 3) and thus, it is not implausible that changing the measure of geography can lead to no longer a significant effect.

6. Moulding natural amenities: waterfront modifications

Results of the previous section indicate that natural amenities are relevant elements behind the heterogeneity of the persistence of redlining. This finding is consistent with extensive literature documenting amenities as sources of persistent spacial differences. The following section departs from such consideration by considering that natural amenities are not immutable but can be shaped through human intervention. A static and unchanging component of geography exists: shores, lakes, and mountains cannot change their physical locations. But,

other components of amenities are susceptible to being changed. For instance, accessibility to water amenities can change with the creation of waterfront promenades. Similarly, the utility generated by amenities can also change rehabilitating abandoned structures or cleanups.

The analysis in this section focuses on waterfront redevelopment plans that have occurred since the 1970s. These redevelopment plans targeted previously industrial or commercial areas that, with the changes in industry location, had been left abandoned, polluted and inaccessible. Examples include Boston's North End, whose waterfront was once a major commercial and industrial area before being abandoned in the 1960s and 1970s. The Baltimore Inner Harbor followed a similar path, losing relevance after the introduction of container ships, which could no longer dock there due to their size. City authorities established a series of redevelopment plans in these areas that included rehabilitating abandoned wharves and structures and creating and improving waterfront access (i.e., the creation of the Christopher Columbus Waterfront Park in North End). Both areas redeveloped quickly as a result of these strategies. These two stories illustrate the possibility of modifying geography and that this intervention can have a strong impact on neighborhood trajectories. Following the success of Baltimore and Boston, other cities in the US have adopted since then similar strategies to redevelop previously industrial waterfront areas. These revitalization plans capture the modifiable aspect of natural amenities, but they are as well examples of policies that can help overcome the legacy of redlining.

In the same fashion as in the previous sections, the relationship between the persistence of redlining, the presence of water natural amenities, and their modifications can be expressed by adding an additional dimension to the diff-in-diff:

$$y_{int} = \beta_0 + \beta_1 R_i + \beta_2 A_i + \beta_3 (R_i \times A_i) + \beta_4 (A_i \times W_i) + \beta_5 (R_i \times A_i \times W_i) + \beta_6 (R_i \times Post^{1977}) + \beta_7 (A_i \times Post^{1977}) + \beta_8 (A_i \times W_i \times Post^{1977}) + \beta_9 (R_i \times A_i \times Post^{1977}) + \beta_{10} (R_i \times A_i \times W_i \times Post^{1977}) + \alpha_{im} + \gamma_t + \epsilon_{int} \quad (3)$$

where W_i is an indicator for waterfront redevelopment projects, and the rest of the variables are defined as in the previous equations⁴². Because modifications only happen in areas with natural amenities, W_i is never included by itself, and only the interactions between A_i and W_i are considered. The coefficient β_{10} represents the catch-up for areas with modified waterfronts compared to the convergence for areas with unmodified natural amenities.

The results of estimating Equation 3 at the within MSA level are shown in Table 6⁴³. The

⁴²Modifications, as defined here, do not take into account the timing. Since these modifications are relevant after the 70s, coefficients that do not interact with the $Post^{1977}$ variable will capture the situation of areas that will experiment a waterfront redevelopment but have not been modified yet.

⁴³Given that modified waterfront were usually industrial or commercial areas that were separated from the rest of the city, affected neighborhoods also tended to be separated or surrounded by D neighborhoods, since these areas were the oldest part of the cities, inhabited by low-income population working on those industries and also because industrial and business "encroachment" were considered an adverse influence for surveyors and were associated with the worst grade. As a result, this equation can only be estimated with the within MSA strategy.

Table 6: Moulding natural amenities

VARIABLES	(1) White Share	(2) % HU above MSA MHV	(3) % Families above MSA MFI
D-graded	-0.133*** (0.0104)	-0.136*** (0.00975)	-0.0944*** (0.00576)
Natural Amenities	0.0205*** (0.00679)	0.0236*** (0.00787)	0.0113*** (0.00406)
D-graded × Natural Amenities	-0.0208 (0.0133)	-0.0641*** (0.0123)	-0.0244*** (0.00729)
Natural Amenities × Modification	0.0445*** (0.0158)	0.00283 (0.0247)	-0.0534*** (0.0114)
D-graded × Natural Amenities × Modification	0.00248 (0.0273)	-0.0632* (0.0327)	-0.0138 (0.0173)
D-graded × Post ¹⁹⁷⁷	0.0589*** (0.0138)	0.0706*** (0.0125)	0.0268*** (0.00772)
Natural Amenities × Post ¹⁹⁷⁷	0.0349*** (0.00997)	0.0148 (0.0101)	0.0174*** (0.00572)
Natural Amenities × Modification × Post ¹⁹⁷⁷	0.0169 (0.0247)	0.131*** (0.0304)	0.0287 (0.0175)
D-graded × Natural Amenities × Post ¹⁹⁷⁷	-0.0173 (0.0177)	0.0202 (0.0158)	-0.00217 (0.00988)
D-graded × Natural Amenities × Modification × Post ¹⁹⁷⁷	0.0704* (0.0370)	0.0942** (0.0406)	0.0839*** (0.0251)
Observations	19,460	19,418	19,454
Year FE	YES	YES	YES
MSA FE	YES	YES	YES
Border-pair FE	NO	NO	NO
Sample	All D-C	All D-C	All D-C
Adjusted Within R-squared	0.0434	0.0658	0.0769
Mean Dep. Var	0.635	0.409	0.429

Robust standard errors in parentheses

*** p<0.01, ** p<0.05, * p<0.1

Notes: This table shows the results from estimating Equation 3 on the MSA D-C sample, for the period 1950-2015. Post¹⁹⁷⁷ is defined from 1980-2015. Natural amenities and modifications are described as in the text. Modification is an indicator for waterfront redevelopment projects (1 if the neighborhood falls within the 500 meter buffer around the project, 0 otherwise).

main implication is that the D-natural amenities-post CRA coefficient is no longer significant, whereas the new interaction with modifications exhibits a stronger and larger convergence. Relative to the convergence for areas with unmodified amenities, the catch-up would be 7 pp higher in terms of share of white population, 9 pp higher for the share of housing units on and above the MSA median value, and 8 pp higher for the share of families on and above the MSA median income. These results indicate that not all amenities drive the effects found in the previous section, but rather the modified ones in an attempt to revitalize them are the ones leading to stronger convergence for redlined areas. In fact, for neighborhoods with waterfront beautification, the gaps get reduced by around 70% for population and housing values and up to 82% for family income, while this reduction remains much lower for areas with no modifications (around 30% for population, 20% for income and 50% for home values).

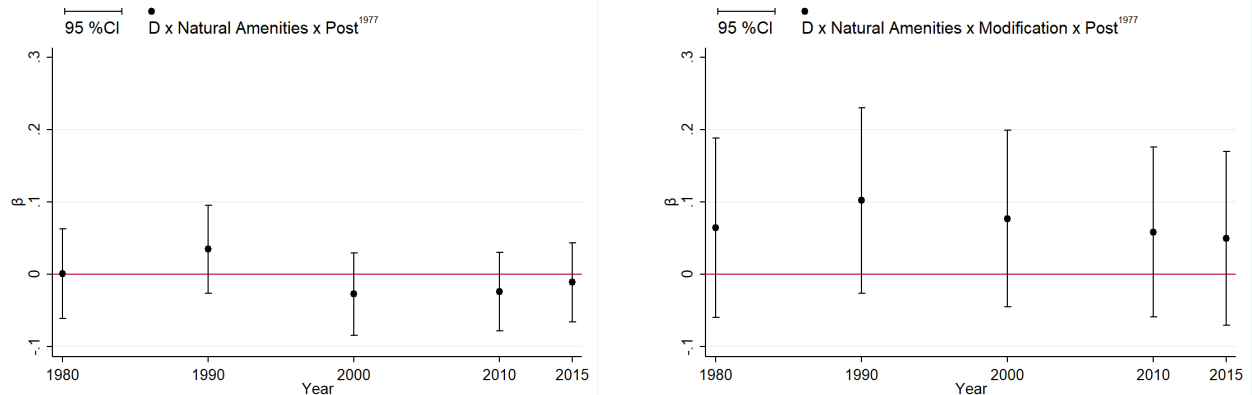
I explore the timing of the effects by modifying Equation 3 in the same way as in the previous sections, by modifying Equation 3. Figure 4 plots the coefficients for the interaction with amenities and modified waterfronts, together with the 95% confidence intervals. This graph reveals two facts. First, except in 1990, there are no significant effects for the interaction with natural amenities alone for any of the variables. Hence, natural amenities per se do not lead to faster catch-up. This is no longer the case when considering the coefficients for interaction with natural amenities and modifications. Most of the coefficients for income and home values are positive and significantly different from zero, even if the effect does not occur immediately after the CRA. The lack of an immediate effect is consistent with the fact that this regression does not account for the timing of the changes. As a result, this time trend shows a gradual-accumulating pattern since it is reflecting when the modifications take place. For white population, the effects of this interaction are concentrated in 1990. The results on white population may be weaker for two reasons. First, because redlined cities tended to have more black population and, thus, convergence at the MSA level can be weaker, as previously discussed. Second, areas with modified waterfronts had also higher shares of white population during redlining, which could be explained if in these industries there was a higher share of white population working and, also, because industries that offer housing arrangements for their workers tended to offer them separately for white and black workers (Rothstein, 2017). The evidence presented here, along with the one in Figure 3, implies that: (1) Convergence in D areas with no amenities has modestly been stagnant, indicating the need for interventions to overcome the legacy of redlining, and (2) given the effects found for waterfront modifications, interventions focusing on this modifiable aspect of amenities to improve convergence in the remaining D areas.

Robustness

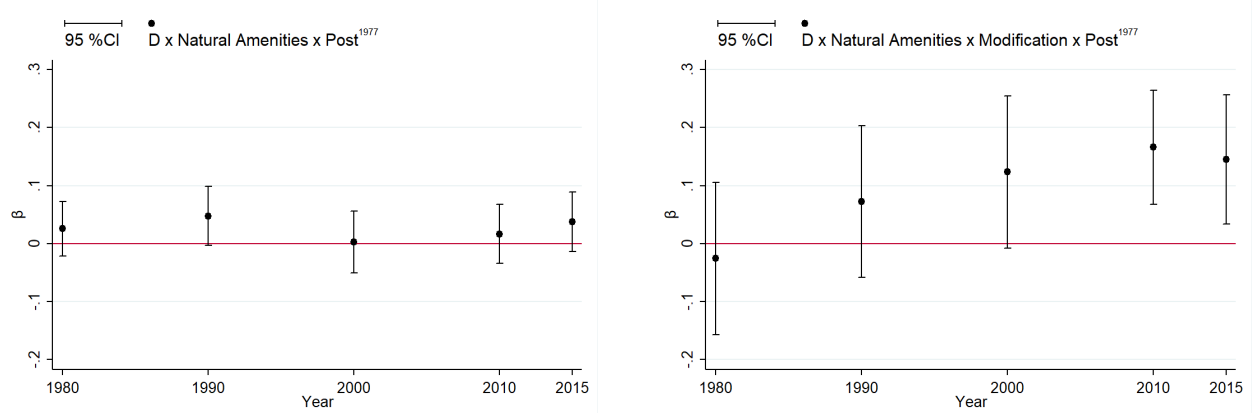
Given that these waterfront modifications have been occurring since the 1970s, the effects may be simply capturing the tendency of natural amenities to change over time. To exclude the possibility, Equation 2 is estimated by adding natural amenities-year fixed effect to eliminate

Figure 4: Natural amenities, waterfront modifications and timing of the effects

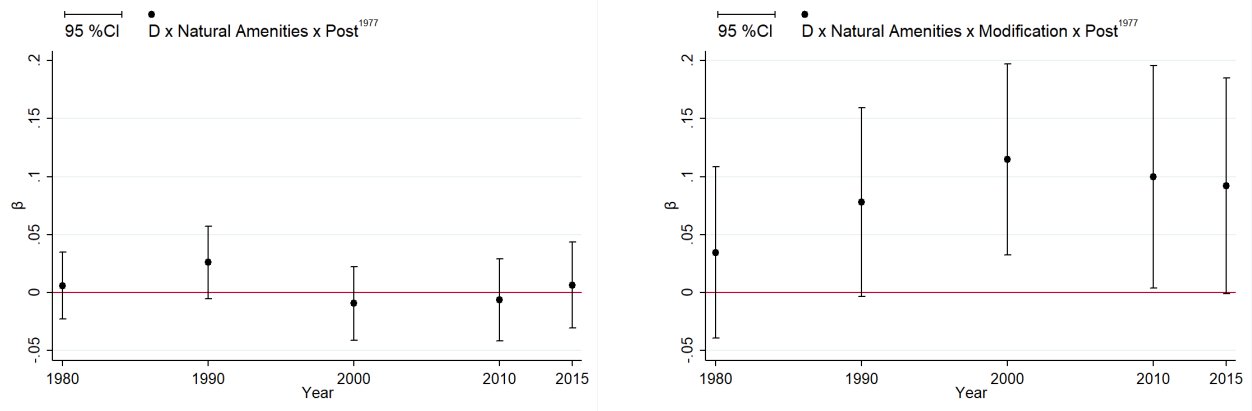
Panel A: White Population



Panel B: Home Values



Panel C: Family Income



Notes: Figure shows the respective coefficients and 95 % CI from estimating Equation 3 where $Post^{1977}$ takes values zero between 1950-1970 and a different value for each decade after the removal of redlining. Estimated on MSA D-C sample. Dependent variables are the same as in Table 6.

variation generated by these tendencies. Appendix Tables 9.3.12 and 9.3.13 show that the previous results remain unchanged even after including these fixed effects to absorb the time-trends⁴⁴. Hence, this tendency does not capture waterfront modifications, and it is reasonable to consider them separately in the analysis. Results in Table 6 are also robust to these fixed effects (not shown).

The definition of modifications used here has the additional problem of not considering the modifications and pooling already modified areas with future modifications. To explore the robustness of the results, I estimate a variation of Equation 3 in which modifications are defined with the same buffer criterion but also with the timing, so that they only appear as they take place. Given that these revitalization projects occurred only after the 70s⁴⁵, I eliminate the variables that are not interacted with the *Post*¹⁹⁷⁷. The results in Appendix Table 9.3.15, are early identical to those of Table 6. The main difference would be stronger effects for white population and slightly weaker effects in terms of home values. Moreover, unmodified natural amenities would lead to faster convergence in home values. Given that the interaction between D-natural amenities-post CRA will capture also areas that will undergo future modifications, one possible explanation is that housing values are forward-looking and thus begin to change ahead of revitalization programs.

Finally, the natural amenities definition includes not only water features but also parks, which are not considered to be modified. I show that the results are robust to the absence of parks by excluding them from the definition of natural amenities so that I only consider the water features that have been modified. Results in Appendix Table 9.3.16 show that the main conclusions remain unchanged even after excluding parks from the definition of natural amenities.

7. Greening redlining

Previous findings have revealed the existence of potential interventions that can alter natural amenities and reverse the effects of redlining. These waterfront redevelopments, however, are only feasible in neighborhoods near such water features. Because it is geographically impossible to implement these policies anywhere, the persistence cannot be modified for neighborhoods lacking such features. This section investigates how changes in a geographically unconstrained amenity, tree canopy, affect D-C gaps using a two-stage least squares strategy.

Due to data limitations, exploring the effects of tree canopy changes on neighborhood outcomes requires a different strategy. Modifying Equation 1 to incorporate changes in tree coverage in a similar fashion as for natural amenities and waterfront modifications is unfeasible given the lack of high-resolution aerial imagery (i.e., $1m^2$ pixels or less) before 2003. Hence, I will consider a snap-shot in time and estimate how outcomes in 2015 differ for D-graded

⁴⁴Notice that in this regression the interaction between natural amenities and post CRA is not included since it would be collinear to the amenities-year fixed effect.

⁴⁵The only exception would be Chicago Front Trail, to which I assigned 1964 because it was the only date found.

Table 7: OLS results

VARIABLES	(1)	(2)	(3)
	White Share	% HU above MSA MHV	% Families above MSA MFI
D-graded	-0.0699*** (0.0181)	-0.0528*** (0.0137)	-0.0857*** (0.0122)
ΔTC	0.0121** (0.00479)	0.0115** (0.00448)	-0.00212 (0.00558)
D-graded $\times \Delta TC$	-0.00232 (0.0103)	0.0103 (0.00721)	0.0104 (0.0103)
Observations	1,384	1,383	1,384
MSA FE	YES	YES	YES
Sample	All D-C in 2015	All D-C in 2015	All D-C in 2015
Adjusted Within R-squared	0.0145	0.0219	0.0389
Mean Dep. Var	0.444	0.380	0.366

Robust standard errors in parentheses

*** p<0.01, ** p<0.05, * p<0.1

Notes: This table shows the results from estimating Equation 4 on the MSA D-C sample. Changes in tree canopy cover the period 2000s-2015. All variables are defined as in the text. Due to the inaccuracy of tree canopy predictions in Los Angeles, Oakland, San Francisco and Chicago, these cities are excluded from the regression.

neighborhoods depending on the experimented change in the tree canopy. Formally, the goal is to estimate:

$$y_{im}^{2015} = \beta_0 + \beta_1 R_i + \beta_2 \Delta TC_i^{2015} + \beta_3 (R_i \times \Delta TC_i^{2015}) + \alpha_{im} + \epsilon_{im} \quad (4)$$

where all variables are defined as before and ΔTC_i^{2015} represents the growth rate of detected tree pixels between the 2000s-2015 (i.e., $\frac{TC_i^{2015} - TC_i^{2000s}}{TC_i^{2000s}}$)⁴⁶. The coefficient of interest in Equation 4 is β_3 since it captures how the D-C gap changes for a 100% increase in tree coverage. Results from estimating Equation 4 are shown in Table 7.

However, estimating Equation 4 with OLS would result in biased estimates because changes in urban trees could be endogenous. First, Equation 4 may be suffering from reverse causality, and increases in tree canopy could be either a cause or a consequence of better neighborhood outcomes. Second, there is potential for omitted variable bias, and unobserved events and local interventions associated with changes in urban green spaces (i.e., new constructions or sidewalks and street renewals) could be biasing the estimates. Third, even though the tree detection algorithm achieves an average precision of 90%, measurement error is unavoidable, and some pixels will be incorrectly labeled. Furthermore, there is evidence that differences in

⁴⁶Due to computational constraints, changes in detected trees can only be measured between two time periods. The first period is labeled 2000s since the first available data year depends on the states and ranges between 2003-2007. For a detailed explanation of data construction, see the following section.

tree canopy are related to redlining, with D-graded areas having lower levels of vegetation cover (Locke et al. (2021), Nardone et al. (2021) and Namin et al. (2020)). Similarly, redlining influences the evolution of tree coverage because D areas tend to meet the criteria for priority plantation sites (i.e., high imperviousness, urban heat islands, social and economic inequality)⁴⁷. Appendix Table 9.3.5 provides additional evidence showing that (1) D neighborhoods are the ones with the lowest share of tree pixels, (2) together with C areas, they are the ones below total average canopy cover and (3) despite of a general increase in tree cover for all neighborhoods, the greatest increase takes place in redlined areas.

To address these endogeneity concerns, this paper employs a two-stages least squares approach and predicts changes in tree coverage with changes in exposure to exotic tree plagues⁴⁸. The exotic plagues used to construct the instrument were discovered to be the deadliest in 2015 (Fei et al., 2019). To further ensure relevance and exogeneity, two plagues with different mortality and management strategies are excluded⁴⁹. The first one is the Gypsy Moth since host mortality occurs only after successive defoliation, which is unobservable using available data, and recent management strategies have focused on mating disruption to slow its spread. The other excluded plague is the White Pine Blister Rust, a pathogen whose relatively long time of latent infection, along with the fact that it spreads through infected ribes and not from tree to tree implied tree removals were ineffective ways of managing the disease (Maloy, 2003). For the considered plagues, chemical treatments, when available, are usually preventive, typically need to be repeated annually or biannually, and due to their costs and ecological impact, are generally only recommended for high-value ornamental tree. As a result, management strategies typically include a combination of hosts removals and preventive treatments when these costs are not expected to rise in an eventual future infection⁵⁰.

Non-native tree plagues are exogenous shocks whose management requires the removal of affected trees and their replacement (Aukema et al. (2011), Hudgins et al. (2022)). Because replacements are determined by the size, species, condition, and location of removed trees in

⁴⁷See the evidence provided by Hoffman et al. (2020) on redlining, imperviousness, and urban heat islands.

⁴⁸Compared to native plagues, exotic ones represent a greater threat due to (i) the limited co-evolution between hosts and plagues that reduces host resistance (Tubby and Webber, 2010) and (ii) the lack of native enemies that facilitates the spread upon arrival (Aukema et al., 2011). Some examples include the Gypsy Moth, accidentally released in the 1860s, and that between 1920-2002 defoliated over 95 million acres (Coleman, Haavik, Foelker, and Liebhold, 2020). The arrival of the Dutch Elm Disease (DED) to Ohio in the 1930s caused similar consequences killing 56 % of the original northeastern in the next 40 years. Other examples include the Hemlock Wolly Adelgid, the Asian Longhorned Beetle, or the recent Emerald Ash Borer. On average, host mortality occurs within 4-10 years of infection of these plagues.

⁴⁹Additionally, four plagues are not detected in the data used. These plagues are the green spruce aphid, the laurel wilt, the sudden-oak death and the Port-Orford-cedar root disease.

⁵⁰Costs increase with the tree basal area (area covered by the stems), whose evolution is closely related to the age of the tree. Typically, young trees and old trees tend to grow slower than middle-aged ones. Therefore, medium-age trees with medium-to-large basal areas are the removed ones whilst young and old trees may be preventively treated.

an attempt to maintain their value, replacement may not be on a one-to-one basis⁵¹. Typically, medium-to-large basal area trees, which are the most vulnerable to removal, must be substituted by more than one smaller tree. Hence, variation in plagues stemming from lengthier exposure and new plagues arrival will trigger an exogenous change in canopy that can be used as an instrumental variable.

Using the data on pests and potential hosts distribution described in Section 3 assumes all neighborhoods within a county infested by plague j are infested if they have pest j hosts, and that exposure is higher the higher area of potential hosts. Letting PH_{ij} be the share of plague j potential hosts basal area to detected trees in 2000 in neighborhood i and Y_{ij}^t the years since the detection of plague j in that area, changes in plague exposure in neighborhood i between 2000-2015 are defined as follows:

$$\Delta PlagueExposure_i^{2015} = \sum_{j=0}^{j=5} PH_{ji}^{2000} \times \Delta Y_{ij}^{2015} \quad (5)$$

Equation 5 captures different sources of variation in exposure: variation in the share of trees potentially infected (PH_{ji}^{2000})⁵², and variation in the years of exposure (Y_{ij}^{2015}). Since particular species may be endogenously allocated to neighborhoods, considering all j plagues combined strengthens the exogeneity of the instrument by capturing susceptibility to any plague rather than a specific one. The inclusion of times of exposure captures that the effect on tree replacements rises with longer exposures as more hosts are affected. Similarly, for trees that were replaced, there must be some time lag before their size is large enough to be detected in imagery.

Then, the first stage equation is defined as:

$$\Delta TC_i^{2015} = \alpha_0 + \alpha_1 R_i + \alpha_2 \Delta PlagueExposure_i^{2015} + \alpha_3 (R_i \times \Delta PlagueExposure_i^{2015}) + \alpha_{im} + u_i \quad (6)$$

where all variables are defined as in the text. Notice that R_i is included since it will appear in the second stage equation and if ΔTC_i is in fact related to R_i but not controlled for, estimating Equation 6 will yield an error term correlated with R_i and biased estimations. Since R_i is uncorrelated with u_i , so is the interaction between R_i and $\Delta PlagueExposure_i^{2015}$. Adding the interaction has the additional advantage of controlling for possible concerns regarding

⁵¹An example can be seen in the New York City Department of Parks & Recreation regulations: <https://www.nycgovparks.org/rules/section-5>. Other more practical examples are available at the Tree Plantation guidelines of Arlington: <https://www.arlingtonva.us/Government/Programs/Building/Resources/Tree-Replacement>. Research suggests that tree replacement based on leaf area would range from 13.7 per large removed tree to 3.3 per small removed tree (Nowak and Aevermann, 2019). Moreover, new plantations can take place with non-host species or genetically resistant hosts (i.e. the pacific hemlock is resistant to plagues affecting the Atlantic one). In fact, for plagues that are considered endemic, research is trying to develop host-resistant species rather than treatments.

⁵²The normalization with pixels detected in the 2000s is done because the increases in tree canopy are also defined relative to these pixels.

heterogeneity in plague effects and management⁵³. Decomposing Equation 6 into fitted values ($\widehat{\Delta TC}_i$) and an error term (ν_i) and plugging this decomposition in Equation 4 yields:

$$y_{im}^{2015} = \beta_0 + \beta_1 R_i + \beta_2 \widehat{\Delta TC}_i^{2015} + \beta_3 (R_i \times \widehat{\Delta TC}_i^{2015}) + \alpha_{im} + \zeta_i \quad (7)$$

where $\zeta_i = \beta_2 \nu_i + \beta_3 (R_i \times \nu_i) + \epsilon_{im}$. Estimating this equation would be problematic if any of the regressors are correlated with the error ζ_i . However, notice that $\widehat{\Delta TC}_i^{2015}$ would be, by construction, orthogonal to both ν_i , ϵ_{im} and R_i and hence uncorrelated with the error. Similarly, R_i will also be uncorrelated to u_i since it is included as a regressor in the first stage and is also orthogonal to ϵ_{im} . The only potential concern would be the correlation between R_i and the term $R_i \times \nu_i$ but since R_i is orthogonal to ν_i and R_i^2 is R_i (i.e., it is a dummy variable), there is no correlation between regressors and ζ_i and hence Equation 7 can be estimated safely⁵⁴.

Given the spatial correlation between species distribution and plagues for neighboring areas, estimating Equation 6 and 7 at the border-pair level is unfeasible, since there would not be enough variation in plague exposure to predict tree canopy after adding border-pair fixed effects.

The underlying assumption behind the use of exotic pests as instruments is that they have an equal effect on all neighborhoods. This assumption is not unrealistic since infected, dead, or at-risk trees, private or public, are equally likely to be removed regardless of the neighborhood if they share similar age and basal area. Since this paper focuses on similarly old neighborhoods, D and C areas, the overall distribution of tree canopy should be akin since they have experienced the same shocks. As a result, changes in exposure to plagues should have comparable effects in both neighborhoods. Other potential threats could be that mortality rates are endogenous due to the environmental stresses for trees caused by redlining or that replacements are endogenous, and D-graded areas receive lower or slower-growth replacement trees. Importantly, these hypotheses can be checked empirically by looking at the estimates of α_1 and α_3 in Equation 6.

Table 8 displays, on Panel A, the results of estimating the first stage equation (Equation 6) and, on Panel B, the results of the second stage (Equation 7). The first stage results show that increases in plague exposure lead to significant increases in tree canopy. To simplify the interpretation of $\Delta PlagueExposure_i^{2015}$, a standard deviation increase in plague exposure leads to 28 pp higher increases in tree coverage. Column (2) of Panel A also controls for natural amenities, their modifications and the interactions with redlining, since the presence of these features could be correlated with the observed changes in tree canopy. The results remain unchanged even after adding these additional controls. Moreover, results do not show significant heterogeneity in the effect of plague exposure for D and C areas, reinforcing the exogeneity of the instrument.

⁵³For instance, given the evidence in Hoffman et al. (2020) on redlining areas suffering from urban heat islands, it could be that trees in redlined areas are subject to more stress and therefore be more likely to die from plagues. These effects, if they exist, will be accounted for by the interaction of both variables.

⁵⁴ $Cov(R_i, R_i \nu_i) = E(R_i^2 \nu_i) = E(R_i \nu_i) = E(R_i)E(\nu_i) = 0$.

Table 8: Greening redlining

Panel A: First stage	(1)	(2)
VARIABLES	Δ Tree canopy	Δ Tree canopy
D-graded	0.115 (0.0972)	0.139 (0.103)
Δ Plague Exposure	51.45*** (2.432)	51.86*** (2.296)
$D\text{-graded} \times \Delta \text{Plague Exposure}$	15.11 (48.49)	6.632 (47.82)
Interpretation		
$\Delta 1 \text{ SD } \Delta \text{Plague Exposure}$	0.28	0.29
Observations	1,386	1,386
MSA FE	YES	YES
D-grade x NA	NO	YES
D-grade x NA x Modification	NO	YES
Sample	All D-C in 2015	All D-C in 2015
F stat	151.3	173.5
Adjusted Within R-squared	0.0288	0.0560
Mean Dep. Var	0.699	0.699

Panel B: Second Stage	(1)	(2)	(3)
VARIABLES	White Share	% HU above MSA MHV	% Families above MSA MFI
D-graded	-0.387*** (0.114)	-0.118 (0.0869)	-0.272*** (0.0691)
$\Delta \widehat{\text{Tree canopy}}$	0.0508* (0.0265)	-0.0102 (0.0136)	0.0204 (0.0172)
$D\text{-graded} \times \Delta \widehat{\text{Tree canopy}}$	0.404*** (0.148)	0.0984 (0.113)	0.249*** (0.0895)
Observations	1,384	1,383	1,384
MSA FE	YES	YES	YES
Sample	All D-C in 2015	All D-C in 2015	All D-C in 2015
Adjusted Within R-squared	0.0240	0.00682	0.0458
Mean Dep. Var	0.444	0.380	0.366

Robust standard errors in parentheses

*** p<0.01, ** p<0.05, * p<0.1

Notes: This table shows the results from estimating Equation 6 (Panel A) on and Equation 7 (Panel B) on the MSA D-C sample. Changes in tree canopy cover the period 2000s-2015. All variables are defined as in the text. Due to the inaccuracy of tree canopy predictions in Los Angeles, Oakland, San Francisco and Chicago, these cities are excluded from the regression.

Comparing the second stage results in Panel B with the OLS results in Table 7 shows that the OLS estimates are downward biased. Moreover, while there are no significant effects for the interaction between D-graded and changes in tree coverage with OLS, the interaction becomes significant and positive for white population and family income using the two-stages least squares strategy: when the tree canopy doubles, the demographic composition, and family income completely converge (i.e., $\beta_1 + \beta_3$ in Equation 7). The lack of a significant effect on home values at the neighborhood level is consistent with the literature on the hedonic analysis of trees. Because the impact of trees on property prices decays with distance, and thus observing only medians of values at the neighborhood level can offset the effect.

The difference between IV and OLS estimates is consistent with Baum-Snow (2007) and Duranton and Turner (2012), suggesting that the increases in tree coverage result from policy interventions in areas that have not converged to achieve the catching-up. The existence of tree plantation and regreening initiatives in low-income areas sustains this hypothesis. For instance, Groundwork USA, a network of approximately 20 local trusts, was founded in 1998 from a partnership between the National Park Service and the Environmental Protection Agency and is devoted to improving the environmental conditions of low-resource communities and reverting the legacy of poverty and discrimination through multiple greening initiatives. Similarly, the Environmental Tree Service in Portland has provided free street trees to low-income and under-served communities since 2008. Moreover, with the publication of the HOLC maps, initiatives also started to focus explicitly on formerly redlined neighborhoods. For instance, the Southside ReLeaf association has been committed to reverting the environmental legacy of redlining in South Richmond since 2019.

Robustness

Given the high difference between OLS and IV estimates, I also estimate the reduced form of Equation 4 introducing changes in plague exposure directly. Results shown in Table 9 corroborate the previous finding: D-graded areas that experiment with higher exposure to plagues have higher shares of white population and family income. Quantifying the effects, one more standard deviation in changes in plague exposure for D-graded areas would lead to a 15 pp higher share of white population and a 9 pp higher share of families above the MSA median family income. Comparing these effects with the D-C gap would imply that a standard deviation increase in plague exposure can lead to complete convergence. As in Table 8, there are no significant effects on housing values. Appendix Table 9.3.17 shows that these results remain unchanged even after controlling for natural amenities, modifications, and their interaction with redlining. Moreover, estimating the second stage controlling for natural amenities, modifications, and the interaction with redlining and using the fitted first-stage values of Column (2) in Panel A Table 8 does not lead to significant differences in the estimates, as shown in Appendix Table 9.3.18.

Table 9: Reduced form results

VARIABLES	(1) White Share	(2) % HU above MSA MHV	(3) % Families above MSA MFI
D-graded	-0.0857*** (0.0168)	-0.0471*** (0.0132)	-0.0872*** (0.0109)
Δ Plague Exposure	2.612* (1.365)	-0.522 (0.698)	1.050 (0.885)
D-graded × Δ Plague Exposure	27.67*** (9.784)	6.395 (7.479)	16.90*** (5.919)
Interpretation:			
D-graded × Δ 1 SD Δ Plague Exposure	0.15	0.03	0.09
Observations	1,384	1,383	1,384
MSA FE	YES	YES	YES
Sample	All D-C in 2015	All D-C in 2015	All D-C in 2015
Adjusted Within R-squared	0.0240	0.00682	0.0458
Mean Dep. Var.	0.444	0.380	0.366
Robust standard errors in parentheses			
*** p<0.01, ** p<0.05, * p<0.1			

Notes: This table shows the results from estimating a reduced form Equation 4 with changes in plague exposure on the MSA D-C sample. Changes in tree canopy cover the period 2000s-2015. All variables are defined as in the text. Due to the inaccuracy of tree canopy predictions in Los Angeles, Oakland, San Francisco and Chicago, these cities are excluded from the regression.

8. Development or displacement?

The results of the previous sections show that waterfront modifications or re-greening strategies result in a nearly complete catch-up. However, these effects could be explained by two contrasting stories with different policy implications. On the one hand, convergence may occur if neighborhood improvements result in higher home values for previously discriminated residents. Residents' welfare would thus improve because they would live in neighborhoods with natural amenities and improved public amenities such as education funded by housing taxes. In this case, waterfront beautifications and re-greening strategies could effectively reverse the consequences of redlining for neighborhoods and individuals. Displacement, on the other hand, could be causing the observed effects. Neighborhoods with altered natural amenities or greened areas, in particular, may be experimenting with large influxes of white people. Increased demand for these neighborhoods would raise housing prices and eventually displace the original residents to areas with similar pre-convergence characteristics or even worse if residents are displaced to areas without natural amenities. As a result, despite successfully allowing D-graded neighborhoods to converge, the policy interventions proposed in this paper would not reduce persistence for individuals.

The empirical requirements to address this issue, which primarily involve observing previous and past residences as well as other socioeconomic outcomes at the individual level, make it difficult to determine what is causing the effects. However, the Opportunity Atlas (Chetty et al., 2018) can be exploited to provide some intuition. This dataset offers information on adulthood outcomes measured around 2015 for children born between 1978 and 1983, right after redlining was made illegal. Changes in geographic and intergenerational mobility can be observed because children's outcomes are linked to parental outcomes. Low geographic mobility of children and improvements in intergenerational mobility would imply that the findings reflect *real* neighborhood improvements. The opposite would indicate that displacement is behind the observed convergence. The goal of this exercise is only to use the Opportunity Atlas data as an approximation to understand the explanation behind my results. As a result, this section builds on Aaronson et al. (2021a)'s work on the causal effects of redlining in intergenerational mobility considering geographic and economic mobility as indicators of the underlying different neighborhood development mechanisms⁵⁵. Results from previous sections showed that the effects on natural amenities started in recent years. Similarly, most of the waterfront modifications are post-1970s. Since the Opportunity Atlas data is for children born between 1978-1983, it is unlikely that natural amenities and beautifications had any significant effect on those generations. Thus, this section will focus on the changes in tree coverage.

⁵⁵The Opportunity Atlas provides estimates for children depending on their parents' income rank. However, crosswalking this data requires observing the number of children with parents from that rank (see Appendix 9.1) and this data is not available. As a result, these results cannot be disaggregated for parental income.

Table 10: Redlining, tree canopy and geographic mobility (I)

VARIABLES	(1) Fraction living in childhood's tract	(2) Fraction living in childhood's CZ	(3) Fraction living in parental address
D-graded	0.00114 (0.0149)	0.0430** (0.0173)	0.0219 (0.0143)
$\widehat{\Delta TC}$	0.00216** (0.000919)	-0.000326 (0.00473)	-0.0115*** (0.00229)
D-graded $\times \widehat{\Delta TC}$	0.00229 (0.0194)	-0.0377* (0.0218)	-0.0221 (0.0184)
Observations	1,385	1,385	1,385
MSA FE	YES	YES	YES
Border-pair FE	NO	NO	NO
Sample	All D-C	All D-C	All D-C
Adjusted Within R-squared	6.44e-05	0.0103	0.00925
Mean Dep. Var.	0.202	0.747	0.189
Robust standard errors in parentheses			
*** p<0.01, ** p<0.05, * p<0.1			

Notes: This table shows the results from estimating $y_{im} = \beta_0 + \beta_1 R_i + \beta_2 \widehat{\Delta TC} + \beta_3 (R_i \times \widehat{\Delta TC}) + \alpha_m + \epsilon_i$, where all variables are defined as in the text. Due to inaccuracies in the tree detection algorithm, Los Angeles, Oakland, San Francisco and Chicago are excluded from the analysis

Table 11: Redlining, tree canopy and geographic mobility (II)

VARIABLES	(1) Fraction living in childhood's tract	(2) Fraction living in childhood's CZ	(3) Fraction living in parental address
Panel A: White children			
D-graded	-0.0154 (0.0209)	0.0306 (0.0206)	-0.0102 (0.0195)
$\widehat{\Delta TC}$	0.0111*** (0.000922)	0.00392 (0.00445)	-0.00742*** (0.00140)
$D\text{-graded} \times \widehat{\Delta TC}$	0.0299 (0.0262)	-0.0325 (0.0238)	0.0151 (0.0243)
Observations	1,250	1,250	1,167
MSA FE	YES	YES	YES
Border-pair FE	NO	NO	NO
Sample	All D-C	All D-C	All D-C
Adjusted Within R-squared	0.00711	-0.00102	-0.000786
Mean Dep. Var.	0.187	0.705	0.159
Panel B: Black children			
D-graded	-0.0288 (0.0295)	-0.00454 (0.0300)	0.00750 (0.0307)
$\widehat{\Delta TC}$	-0.0160*** (0.00111)	-0.0108*** (0.00226)	-0.0219*** (0.000860)
$D\text{-graded} \times \widehat{\Delta TC}$	0.0459 (0.0389)	0.0205 (0.0394)	-0.0105 (0.0404)
Observations	1,227	1,227	1,178
MSA FE	YES	YES	YES
Border-pair FE	NO	NO	NO
Sample	All D-C	All D-C	All D-C
Adjusted Within R-squared	0.00871	0.00624	0.0162
Mean Dep. Var.	0.197	0.761	0.199

Robust standard errors in parentheses

*** p<0.01, ** p<0.05, * p<0.1

Notes: This table shows the results from estimating $y_{im} = \beta_0 + \beta_1 R_i + \beta_2 \widehat{\Delta TC} + \beta_3 (R_i \times \widehat{\Delta TC}) + \alpha_m + \epsilon_i$, where all variables are defined as in the text. Due to inaccuracies in the tree detection algorithm, Los Angeles, Oakland, San Francisco and Chicago are excluded from the analysis.

Table 12: Redlining, tree canopy and economic mobility (I)

VARIABLES	(1)	(2)	(3)
	Fraction currently in low poverty neighborhoods	Pr. of reaching 20 %	Mean earnings ptile rank
D-graded	-0.256*** (0.0683)	-0.125*** (0.0332)	-0.0889*** (0.0207)
$\widehat{\Delta TC}$	0.00626 (0.0144)	0.0175* (0.00923)	0.0119* (0.00626)
$D\text{-graded} \times \widehat{\Delta TC}$	0.245*** (0.0899)	0.114*** (0.0438)	0.0704*** (0.0269)
Observations	1,385	1,385	1,385
MSA FE	YES	YES	YES
Border-pair FE	NO	NO	NO
Sample	All D-C	All D-C	All D-C
Adjusted Within R-squared	0.0553	0.0557	0.0710
Mean Dep. Var.	0.361	0.167	0.458

Robust standard errors in parentheses

*** p<0.01, ** p<0.05, * p<0.1

Notes: This table shows the results from estimating $y_{im} = \beta_0 + \beta_1 R_i + \beta_2 \widehat{\Delta TC} + \beta_3 (R_i \times \widehat{\Delta TC}) + \alpha_m + \epsilon_i$, where all variables are defined as in the text. Due to inaccuracies in the tree detection algorithm, Los Angeles, Oakland, San Francisco and Chicago are excluded from the analysis

This section incorporates changes in tree canopy using the two-stages least square described in Section 7. Tables 10, 11, 12 and 13 show the results. Results in Table 10 show that exogenous increases in tree canopy only produce significant differences in geographic mobility for C-graded neighborhoods: doubling the tree canopy leads to a 0.2pp higher share of children who live in their childhood neighborhood. This increase, however, is driven by white population staying: for black population, a 100% increase in tree coverage leads to a 1pp lower fraction remaining in their original tract or commuting zone, as shown in Table 11. These findings suggest that increases in tree coverage result in a significant and geographically extended displacement of black people in C-graded areas, but not of white people, who may remain in the neighborhood.

On the other hand, increasing the urban tree canopy has different effects on economic mobility. Table 12 shows that different from geographic mobility, economic mobility is significantly lower in D-rated neighborhoods. However, the interaction between predicted increases in tree coverage and D-grade is positive and significant: doubling tree coverage would close these gaps. Table 13 shows that the estimates of this interaction differ for black and white populations. While doubling the tree canopy in D-graded neighborhoods increases significantly the fraction of white people in low-poverty areas and the expected income rank, it enlarges the D-C differences for the black population. The observed displacement in the black population in C-graded areas experimenting with increases in tree coverage does not translate to worse

Table 13: Redlining, tree canopy and economic mobility (II)

VARIABLES	(1) Fraction currently in low poverty neighborhoods	(2) Pr. of reaching 20 %	(3) Mean earnings ptile rank
Panel A: White children			
D-graded	-0.195*** (0.0580)	-0.0734** (0.0338)	-0.0665*** (0.0217)
$\widehat{\Delta TC}$	-0.00735 (0.00933)	0.0117* (0.00669)	0.00831* (0.00452)
$D\text{-graded} \times \widehat{\Delta TC}$	0.197*** (0.0752)	0.0578 (0.0430)	0.0490* (0.0268)
Observations	1,250	1,250	1,250
MSA FE	YES	YES	YES
Border-pair FE	NO	NO	NO
Sample	All D-C	All D-C	All D-C
Adjusted Within R-squared	0.0350	0.0219	0.0357
Mean Dep. Var.	0.486	0.230	0.511
Panel B: Black children			
D-graded	0.0238 (0.0249)	0.00704 (0.0205)	0.0215* (0.0112)
$\widehat{\Delta TC}$	-0.0140*** (0.00163)	0.0212*** (0.000805)	0.0133*** (0.000540)
$D\text{-graded} \times \widehat{\Delta TC}$	-0.0803** (0.0316)	-0.0311 (0.0266)	-0.0542*** (0.0141)
Observations	1,227	1,227	1,227
MSA FE	YES	YES	YES
Border-pair FE	NO	NO	NO
Sample	All D-C	All D-C	All D-C
Adjusted Within R-squared	0.0439	0.0428	0.0551
Mean Dep. Var.	0.238	0.103	0.412

Robust standard errors in parentheses

*** p<0.01, ** p<0.05, * p<0.1

Notes: This table shows the results from estimating $y_{im} = \beta_0 + \beta_1 R_i + \beta_2 \widehat{\Delta TC} + \beta_3 (R_i \times \widehat{\Delta TC}) + \alpha_m + \epsilon_i$, where all variables are defined as in the text. Due to inaccuracies in the tree detection algorithm, Los Angeles, Oakland, San Francisco and Chicago are excluded from the analysis.

adulthood prospects for black population in terms of probability of reaching the top 20% or expected income rank. This suggests that increases in tree coverage lead to the displacement of some black residents, but it may benefit stayers in terms of future economic prospects. The evidence in this section suggests that the improvements in neighborhood trajectories obtained from increases in the tree canopy are associated with *gentrification* for black residents. Thus, despite their effectiveness, greening interventions hurt displaced black residents.

9. Conclusion

In response to the mortgage and housing crisis that followed the Great Depression, the New Deal administration undertook a series of reforms that had long-lasting consequences on these sectors. Among them, are the creation of the Home Owner's Loan Corporation (HOLC) and the implementation of the *City Survey Program*. Under this plan, the HOLC graded neighborhoods in US cities with a population greater than 40,000 inhabitants to assess the risk that insuring mortgages supposed for the Federal Government in each neighborhood. The purpose was to devise a system that would allow to guarantee and control the value of the housing assets held by the government through mortgage insurance and refinancing. Following the criteria of the FHLBB Appraisal Manual, neighborhoods could be assigned different grades (A-B-C-D) depending on the transportation access, proximity to amenities, housing, economic, demographic, and racial characteristics of the area. These grades were then represented with different colors (green-blue-yellow-red, respectively) in the *Residential Security Maps*, commonly known as redlining maps. The appraisal criteria reflected the institutionalized racism of the period, leading to minority, black and poor neighborhoods receiving the worst grade (D-graded). Neighborhoods in the worst category were deemed risky and hence deprived of federal housing credit until 1977, with the passing of the Community Reinvestment Act. This practice of systematically denying credit based on neighborhood characteristics is commonly known as redlining. The recent digitization of these maps (Nelson et al. (2017)) opened the path for the study on the long term consequences of this discriminatory lending practices that shows redlining has had persistent effects (Appel and Nickerson (2016), Krimmel (2018), Aaronson et al. (2021b)).

Using the digitized redlining maps, Census data, and the location of water and park amenities for the 1940-2015 period, this paper tries to identify the relationship between the persistence of redlining and natural amenities. Introducing waterfront revitalization projects departs from the traditional view in the literature that considers natural amenities as static and neglects that there is a modifiable dimension. In this way, this paper not only contributes to the above-quoted literature on the persistence of redlining but also to the literature that focuses on natural amenities as determinants of neighborhood outcomes (Rappaport and Sachs (2003); Rappaport (2007); Villarreal (2014); Lee and Lin (2018); Heblitch et al. (2021)). Given the limited geographic span of waterfront beautification projects, this paper also explores how changes in

urban green coverage can mediate the effects of redlining. Hence, this paper also contributes to the literature on the effects of urban tree coverage with the development of new neighborhood panel data on tree canopy and a new instrumentation strategy to tackle the endogeneity behind changes in the tree canopy.

To overcome the selection concerns of the grading process, the empirical strategy implements a diff-in-diff comparing neighborhoods with the most severe credit restriction (D-graded, redlined) to nearby areas with the second worst grade (C-graded, yellowlined). D and C areas had the most similar housing and demographic characteristics but faced different credit policies (i.e., a complete credit restriction vs. a restrictive and conservative lending policy). Moreover, focusing on nearby D-C pairs leverages the new procedure to match redlining maps with Census data here developed, the Census-to-Redlining Constant Crosswalks. The new set of crosswalks constructs data at the originally mapped neighborhood. By assigning Census units to graded neighborhoods, rather than assigning grades to Census units as the literature had previously done, the crosswalks exploit the original sudden change in grades for adjacent areas while preserving the gradual change in unobservables at the D-C border.

The results show that significant gaps between D-C areas have persisted decades after outlawing redlining but that the persistence is heterogeneous and that areas that lie by water and park natural amenities experiment greater convergence in population and housing values to their yellow counterparts. When waterfront revitalization projects are included in the analysis, the results indicate that modified natural amenities are responsible for the greater convergence, as unmodified natural amenities no longer have significant effects. These results show that not all the amenities are enough to overcome the persistence of redlining. Those amenities that have been made accessible to neighborhoods are the ones that allow them to overcome these effects. With these findings in mind, policy interventions focusing on the revitalization of degraded waterfronts can be an effective way to free redlined neighborhoods from the legacy of 40 years of discriminatory lending policies. Finally, the results also show that exogenous increases in tree coverage can completely close the D-C gaps in population and income. However, the increases in tree coverage are also associated with displacement and worse outcomes for the formerly redlined black communities.

This paper demonstrated that not all D-graded neighborhoods remained degraded. Areas with natural amenities can overcome the persistence of redlining much faster. The heterogeneity documented here implies that redlining is not affecting all the residents of previously redlining areas in the same way nowadays. As a result, policy interventions should focus on the degraded ones. Interventions on natural amenities, such as waterfront modifications or increases in the tree canopy, have been shown to be effective ways of reversing the long-run effects of credit restrictions. This last piece of evidence, together with the effects these interventions have on geographic and economic mobility, can be taken as a departure point to study policy interventions aiming to overcome the legacy of redlining.

References

- Daniel Aaronson, Jacob Faber, Daniel Hartley, Bhashkar Mazumder, and Patrick Sharkey. The long-run effects of the 1930s holc “redlining” maps on place-based measures of economic opportunity and socioeconomic success. *Regional Science and Urban Economics*, 86: 103622, 2021a. ISSN 0166-0462. doi: 10.1016/j.regsciurbeco.2020.103622. URL <https://www.sciencedirect.com/science/article/pii/S0166046220303070>.
- Daniel Aaronson, Daniel Hartley, and Bhashkar Mazumder. The effects of the 1930s holc “redlining” maps. *American Economic Journal: Economic Policy*, 13(4):355–92, 2021b.
- Gabriel M. Ahlfeldt, Stephen J. Redding, Daniel M. Sturm, and Nikolaus Wolf. The economics of density: Evidence from the berlin wall. *Econometrica*, 83(6):2127–2189, 2015. doi: 10.3982/ecta10876.
- Attila Ambrus, Erica Field, and Robert Gonzalez. Loss in the time of cholera: Long-run impact of a disease epidemic on the urban landscape. *American Economic Review*, 110(2):475–525, February 2020. doi: 10.1257/aer.20190759. URL <https://www.aeaweb.org/articles?id=10.1257/aer.20190759>.
- Ian Appel and Jordan Nickerson. Pockets of poverty: The long-term effects of redlining. 2016. doi: 10.2139/ssrn.2852856.
- Julian E. Aukema, Brian Leung, Kent Kovacs, Corey Chivers, Kerry O. Britton, Jeffrey Englin, Susan J. Frankel, Robert G. Haight, Thomas P. Holmes, Andrew M. Liebhold, et al. Economic impacts of non-native forest insects in the continental united states. *PLoS one*, 6(9):e24587, 2011. doi: 10.1371/journal.pone.0024587.
- Nathaniel Baum-Snow. Did Highways Cause Suburbanization?*. *The Quarterly Journal of Economics*, 122(2):775–805, 05 2007. ISSN 0033-5533. doi: 10.1162/qjec.122.2.775. URL <https://doi.org/10.1162/qjec.122.2.775>.
- Hoyt Bleakley and Jeffrey Lin. Portage and path dependence. *The quarterly journal of economics*, 127(2):587–644, 2012. doi: 10.1093/qje/qjs011.
- Martí Bosch. Detectree: Tree detection from aerial imagery in python. *Journal of Open Source Software*, 5(50):2172, 2020. doi: 10.21105/joss.02172.
- Leah Boustan, Devin Bunten, and Owen Hearey. Urbanization in american economic history, 1800-2000. *The Oxford Handbook of American Economic History*, 2:75, 2018. doi: 10.1093/oxfordhb/9780190882624.013.25.
- Steven Brakman, Harry Garretsen, and Marc Schramm. The strategic bombing of german cities during world war ii and its impact on city growth. *Journal of Economic Geography*, 4(2):201–218, 2004. doi: 10.1093/jeg/4.2.201.
- Jan K. Brueckner, Jacques-Francois Thisse, and Yves Zenou. Why is central paris rich and downtown detroit poor?: An amenity-based theory. *European economic review*, 43(1):91–107, 1999.
- Raj Chetty, John N. Friedman, Nathaniel Hendren, Maggie R. Jones, and Sonya R. Porter. The opportunity atlas: Mapping the childhood roots of social mobility. Technical report, National Bureau of Economic Research, 2018.

Tom W. Coleman, Laurel J. Haavik, Chris Foelker, and Andrew M. Liebhold. Gypsy moth. *Forest Insect and Disease Leaflet 162. US Department of Agriculture, Forest Service.* 20 p., 2020.

John L. Crompton and Sarah Nicholls. The impact of park views on property values. *Leisure Sciences*, 0(0):1–13, 2019. doi: 10.1080/01490400.2019.1703125.

Kristen B. Crossney and David W. Bartelt. Residential security, risk, and race: The home owners' loan corporation and mortgage access in two cities. *Urban Geography*, 26(8):707–736, 2005. doi: 10.2747/0272-3638.26.8.707.

David Cuberes and Rafael González-Val. The effect of the spanish reconquest on iberian cities. *The Annals of Regional Science*, 58(3):375–416, 2017. doi: 10.1007/s00168-017-0810-0.

Donald R. Davis and David E. Weinstein. Bones, bombs, and break points: the geography of economic activity. *American Economic Review*, 92(5):1269–1289, 2002. doi: 10.1257/000282802762024502.

Gilles Duranton and Matthew A. Turner. Urban Growth and Transportation. *The Review of Economic Studies*, 79(4):1407–1440, 03 2012. ISSN 0034-6527. doi: 10.1093/restud/rds010. URL <https://doi.org/10.1093/restud/rds010>.

Songlin Fei, Randall S. Morin, Christopher M. Oswalt, and Andrew M. Liebhold. Biomass losses resulting from insect and disease invasions in us forests. *Proceedings of the National Academy of Sciences*, 116(35):17371–17376, 2019. ISSN 0027-8424. doi: 10.1073/pnas.1820601116. URL <https://www.pnas.org/content/116/35/17371>.

FHA. Underwriting manual: Underwriting analysis under title ii, section 203 of the national housing act, 1936.

Price Fishback. Panel discussion on saving the neighborhood: Part iii. 2014.

Price Fishback, Jonathan Rose, Ken Snowden, and Thomas Storrs. New evidence on redlining by federal housing programs in the 1930s. *Journal of Urban Economics*, page 103462, 2022. ISSN 0094-1190. doi: <https://doi.org/10.1016/j.jue.2022.103462>. URL <https://www.sciencedirect.com/science/article/pii/S0094119022000390>.

Sofia F. Franco and Jacob L. Macdonald. Measurement and valuation of urban greenness: Remote sensing and hedonic applications to lisbon, portugal. *Regional Science and Urban Economics*, 72:156–180, 2018. ISSN 0166-0462. doi: 10.1016/j.regsciurbeco.2017.03.002. URL <https://www.sciencedirect.com/science/article/pii/S0166046216302708>. New Advances in Spatial Econometrics: Interactions Matter.

James Greer. The home owners' loan corporation and the development of the residential security maps. *Journal of Urban History*, 39(2):275–296, 2013. doi: 10.1177/0096144212436724.

Lu Han, Stephan Heblisch, Christopher Timmins, and Yanos Zylberberg. Cool cities: The value of green infrastructure. 2021.

C. Lowell Harriss et al. History and policies of the home owners' loan corporation. *NBER Books*, 1951. doi: 10.2307/3159550.

Stephan Heblisch, Alex Trew, and Yanos Zylberberg. East-side story: Historical pollution and persistent neighborhood sorting. *Journal of Political Economy*, 129(5):1508–1552, 2021. doi: 10.1086/713101. URL <https://doi.org/10.1086/713101>.

Amy E. Hillier. Redlining and the home owners' loan corporation. *Journal of Urban History*, 29(4):394–420, 2003. doi: 10.1177/0096144203029004002.

Amy E. Hillier. Residential security maps and neighborhood appraisals: The home owners' loan corporation and the case of philadelphia. *Social Science History*, 29(2):207–233, 2005. doi: 10.1017/s014555320001292x.

Jeremy S. Hoffman, Vivek Shandas, and Nicholas Pendleton. The effects of historical housing policies on resident exposure to intra-urban heat: A study of 108 us urban areas. *Climate*, 8(1), 2020. ISSN 2225-1154. doi: 10.3390/cli8010012. URL <https://www.mdpi.com/2225-1154/8/1/12>.

Meghan T. Holtan, Susan L. Dieterlen, and William C. Sullivan. Social life under cover: Tree canopy and social capital in baltimore, maryland. *Environment and Behavior*, 47(5):502–525, 2015. doi: 10.1177/0013916513518064.

Emma J. Hudgins, Frank H. Koch, Mark J. Ambrose, and Brian Leung. Hotspots of pest-induced us urban tree death, 2020-2050. *bioRxiv*, 2022. doi: 10.1101/2021.04.24.441210. URL <https://www.biorxiv.org/content/early/2022/01/23/2021.04.24.441210>.

Disa M Hynsjö and Luca Perdoni. The effects of federal “redlining” maps: A novel estimation strategy. 2022.

Keith R. Ihlanfeldt. The effect of land use regulation on housing and land prices. *Journal of Urban Economics*, 61(3):420–435, 2007. doi: 10.1016/j.jue.2006.09.003.

Kenneth T. Jackson. Race, ethnicity, and real estate appraisal: The home owners loan corporation and the federal housing administration. *Journal of Urban History*, 6(4):419–452, 1980. doi: 10.1177/009614428000600404.

Kenneth T. Jackson. *Crabgrass frontier: The suburbanization of the United States*. Oxford University Press, 1987. doi: 10.2307/493138.

Michelle C. Kondo, SeungHoon Han, Geoffrey H. Donovan, and John M. MacDonald. The association between urban trees and crime: Evidence from the spread of the emerald ash borer in cincinnati. *Landscape and Urban Planning*, 157:193–199, 2017. ISSN 0169-2046. doi: 10.1016/j.landurbplan.2016.07.003. URL <https://www.sciencedirect.com/science/article/pii/S016920461630127X>.

Jacob Krimmel. Persistence of prejudice: Estimating the long term effects of redlining. 2018. doi: 10.31235/osf.io/jdmq9.

Sanghoon Lee and Jeffrey Lin. Natural amenities, neighbourhood dynamics, and persistence in the spatial distribution of income. *The Review of Economic Studies*, 85(1):663–694, 2018.

D. H. Locke, B. Hall, J.M. Grove, et al. Residential housing segregation and urban tree canopy in 37 us cities. *npj Urban Sustainability*, 1(1), 2021. doi: 10.1038/s42949-021-00022-0.

Otis C. Maloy. White pine blister rust. *The Plant Health Instructor*, 2003. doi: 10.1094/phi-i-2003-0908-01. URL <https://www.apsnet.org/edcenter/disandpath/fungalbasidio/pdlessons/Pages/WhitePine.aspx>.

Edward Miguel and Gerard Roland. The long-run impact of bombing vietnam. *Journal of development Economics*, 96(1):1–15, 2011. doi: 10.1016/j.jdeveco.2010.07.004.

Bruce Mitchell and Juan Franco. Holc “redlining” maps: The persistent structure of segregation and economic inequality. *NCRC Research*, 2018.

Dominic J. Morales. The contribution of trees to residential property value. *Journal of Arboriculture*, 6(11):305–308, 1980.

S. Namin, W. Xu, Y. Zhou, and K. Beyer. The legacy of the home owners’ loan corporation and the political ecology of urban trees and air pollution in the united states. *Social Science & Medicine*, 246:112758, 2020. ISSN 0277-9536. doi: 10.1016/j.socscimed.2019.112758. URL <https://www.sciencedirect.com/science/article/pii/S0277953619307531>.

Anthony Nardone, Kara E. Rudolph, Rachel Morello-Frosch, and Joan A. Casey. Redlines and greenspace: The relationship between historical redlining and 2010 greenspace across the united states. *Environmental health perspectives*, 129(1):017006, 2021. doi: 10.1289/ehp7495.

Robert K. Nelson, LaDale Winling, Richard Marciano, Nathan Connolly, et al. Mapping inequality. *American panorama*, 2017. doi: 10.4324/9781315099781-29.

Noelwah R. Netusil, Sudip Chattopadhyay, and Kent F. Kovacs. Estimating the demand for tree canopy: a second-stage hedonic price analysis in portland, oregon. *Land Economics*, 86(2): 281–293, 2010. doi: 10.3368/le.86.2.281.

Tom Nicholas and Anna Scherbina. Real estate prices during the roaring twenties and the great depression. *Real Estate Economics*, 41(2):278–309, 2013.

David J Nowak and Tim Aevermann. Tree compensation rates: Compensating for the loss of future tree values. *Urban Forestry & Urban Greening*, 41:93–103, 2019.

Ben Ost, Weixiang Pan, and Douglas Webber. The returns to college persistence for marginal students: Regression discontinuity evidence from university dismissal policies. *Journal of Labor Economics*, 36(3):779–805, 2018. doi: 10.1086/696204.

Ram Pandit, Maksym Polyakov, and Rohan Sadler. Valuing public and private urban tree canopy cover. *Australian Journal of Agricultural and Resource Economics*, 58(3):453–470, 2014. doi: 10.1111/1467-8489.12037.

Jordan Rappaport. Moving to nice weather. *Regional Science and Urban Economics*, 37(3):375–398, 2007. doi: 10.1016/j.regsciurbeco.2006.11.004.

Jordan Rappaport and Jeffrey Sachs. The united states as a coastal nation. *Journal of Economic Growth*, 8:5–46, February 2003. doi: 10.1023/A:1022870216673.

Richard Rothstein. *The color of law: A forgotten history of how our government segregated America*. Liveright Publishing, 2017.

Allison Shertzer, Tate Twinam, and Randall P. Walsh. Race, ethnicity, and discriminatory zoning. *American Economic Journal: Applied Economics*, 8(3):217–46, 2016. doi: 10.1257/app.20140430.

Allison Shertzer, Tate Twinam, and Randall P. Walsh. Zoning and the economic geography of cities. *Journal of Urban Economics*, 105:20–39, 2018. doi: 10.1016/j.jue.2018.01.006.

K. V. Tubby and J. F. Webber. Pests and diseases threatening urban trees under a changing climate. *Forestry: An International Journal of Forest Research*, 83(4):451–459, October 2010. ISSN 0015-752X. doi: 10.1093/forestry/cpq027.

Tate Twinam. Danger zone: Land use and the geography of neighborhood crime. *Journal of Urban Economics*, 100:104–119, 2017. doi: 10.1016/j.jue.2017.05.006.

Tate Twinam. The long-run impact of zoning: Institutional hysteresis and durable capital in seattle, 1920–2015. *Regional Science and Urban Economics*, 73:155–169, 2018. doi: 10.1016/j.regsciurbeco.2018.08.004.

Carlos Villarreal. Where the other half lives: Evidence on the origin and persistence of poor neighborhoods from new york city 1830-2012. *Unpublished MS.* <https://sites.google.com/site/carlosrvillarreal>, 1(2):3, 2014.

Susan M. Wachter and Grace Wong. What is a tree worth? green-city strategies, signaling and housing prices. *Real Estate Economics*, 36(2):213–239, 2008. doi: 10.1111/j.1540-6229.2008.00212.x.

David C. Wheelock et al. The federal response to home mortgage distress: Lessons from the great depression. *REVIEW-FEDERAL RESERVE BANK OF SAINT LOUIS*, 90(3):133, 2008. doi: 10.20955/r.90.133-148.

Barry T. Wilson, Andrew J. Lister, Rachel I. Riemann, and Douglas M. Griffith. Live tree species basal area of the contiguous united states (2000-2009). 2013.

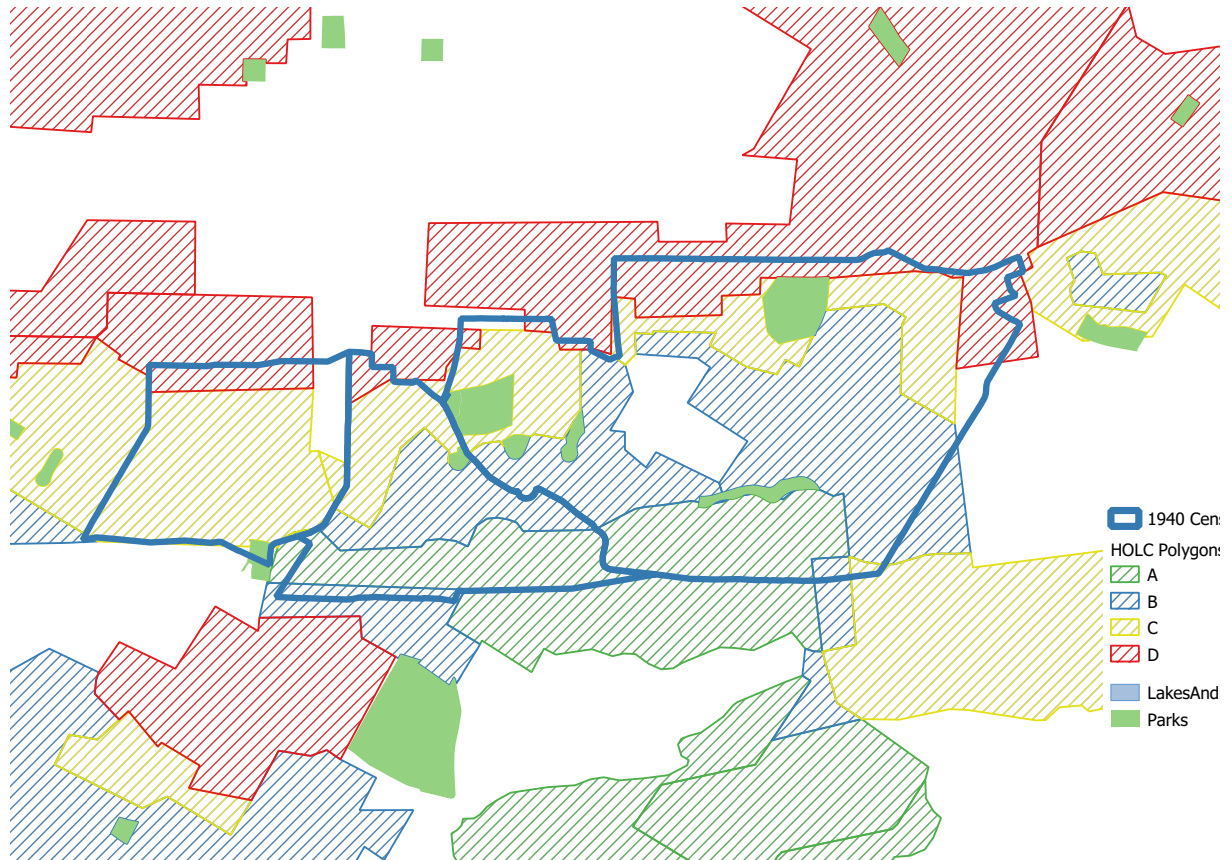
Louis Lee Woods. The federal home loan bank board, redlining, and the national proliferation of racial lending discrimination, 1921–1950. *Journal of Urban History*, 38(6):1036–1059, 2012. doi: 10.1177/0096144211435126.

Lin Yang, Xiaqing Wu, Emil Praun, and Xiaoxu Ma. Tree detection from aerial imagery. In *Proceedings of the 17th ACM SIGSPATIAL International Conference on Advances in Geographic Information Systems*, GIS '09, pages 131–137, New York, NY, USA, 2009. Association for Computing Machinery. ISBN 9781605586496. doi: 10.1145/1653771.1653792.

Appendix

9.1 Census-to-Redlining Constant Crosswalks

Figure 9.1.1: Redlining maps and 1940 tracts



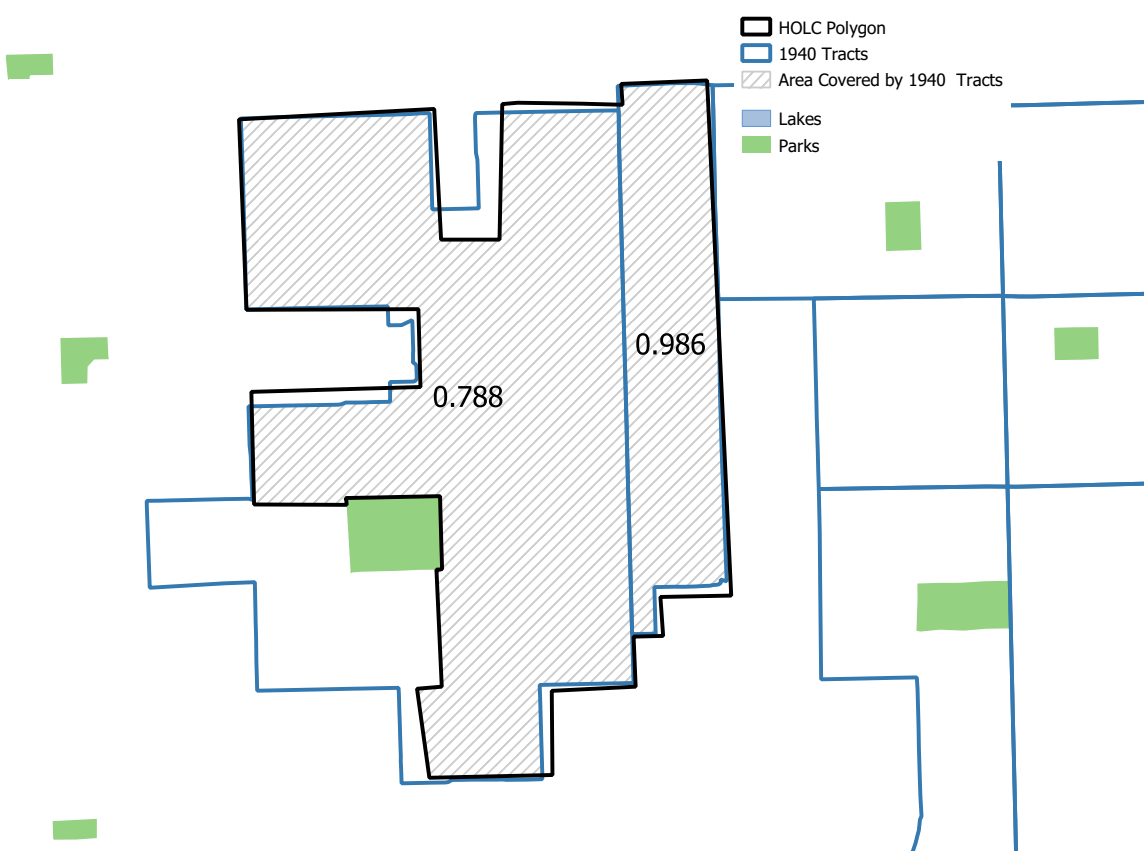
Notes: This figure shows the intersection between HOLC graded neighborhoods from the redlining maps and the 1940 Census tracts. Own elaboration.

As shown in Figure 9.1.1, Census units do not align perfectly with the original neighborhoods of the redlining maps. As a result, one needs to develop a matching method to merge redlining and Census information. As discussed in the main text, assigning grades to Census units generates a series of problems that undermine the validity of the results obtained with that procedure⁵⁶. As a result, I follow the opposite strategy and assign Census units to graded neighborhoods by using the Census-to-Redlining Constant Crosswalks, that I describe in detail in this Appendix.

The basic idea behind the crosswalks is to compute the share of the Census units that falls in the original graded neighborhood. Then, one can use these weights to construct data at the originally graded neighborhood. As shown in Figure 9.1.2, the black line represents the graded neighborhood (HOLC polygon) and the blue line the two tracts that intersect it. For one

⁵⁶This procedure allows to eliminate the measurement error on the grade assignment but the concern of measurement error induced on the neighborhood Census variables by the areal weights would still be present. However, when performing regressions this measurement error will not bias the results as long as it is uncorrelated with the error term.

Figure 9.1.2: Census-to-Redlining Constant Crosswalks



Notes: This figure an example of the areal weights used in the Census-to-Redlining Constant Crosswalks. Own elaboration.

of them 78% of its area is contained in the neighborhood. For the other, 98% of it falls in the neighborhood. As a result, data at the graded neighborhood level will be the weighted sum of the data for these two tracts, with these areal weights.

In order to construct these weights, I first eliminate the area of tracts/block groups and graded neighborhoods that is covered by parks and lakes and compute their areas. The underlying assumption would then be that population is spread homogeneously in the Census units and graded neighborhood once I eliminate the areas that are covered by lakes and parks. Given that there is no population density data for 1940-2015, this is the only source of ancillary information to make the crosswalks more accurate here used. Every HOLC graded neighborhood is given a reference identifier called index, Census units are identified by the GISJOIN code attached to them by the National Register of Historical Places.

Constructing the weights for 1940 is straightforward and is simply done by intersecting 1940 tracts with the originally graded neighborhoods. Then, I compute the area of the intersection. The result will be a file that contains for each graded neighborhood, its area, the tracts that intersect them and their area, and the area of the intersection. From this, I first compute the share of the HOLC neighborhood that is covered by 1940 tracts and keep only the ones that are covered by at least 80%. Then, I simply compute the share of the tract that falls in the neighborhood. For the rest of the years, the process is essentially the same but it becomes more cumbersome since I need to restrict the area to the one covered in 1940. I will use 1950 tracts

for the explanation for simplicity but this is the procedure applied to any other decade besides 1940. In order to do this, I perform the same intersection between 1950 tracts and the HOLC graded neighborhoods. Then, I re-intersect this with the 1940-HOLC intersection. Computing the areas of these re-intersection tells the area of the 1950 tract that was covered already in 1940. Then I simply compute the share of the 1950 tract that falls in this re-intersection area. Since a 1950 tract does not necessarily intersect with only one 1940 tract, I then sum the different weights of the 1950 tract that falls in the same graded neighborhood (i.e., I am just adding the area share of the 1950 tract that corresponds to a 1940 tract and the area share of these same tract that corresponds to other 1940 tract that fall in the same graded neighborhood).

The result from applying this procedure every decade is a set of files that have four columns: the HOLC neighborhood (index), the assigned HOLC grade (A-B-C-D), the identifier for the tract/block group that falls in it (GISJOIN) and the area share of the tract/block group that corresponds to that Census unit-HOLC neighborhood intersection. Then, to construct data at the neighborhood level, one only needs to download data from the National Register of Historical Places at the tract level (1940-1980) and block group level at the (1990-2015). The use of the crosswalks is essentially the same to the use of Lee and Lin (2018)'s ones. However, I will provide an example that also serves as clarification on how the variables in this paper have been constructed.

1. Merge the Census data with the Census-to-Redlining Constant Crosswalks

```
import delimited "$data\NHGIS_1940.csv", rowrange(1:) varnames(1) clear
rename gisjoin gisjoin1940
merge 1:m gisjoin1940 using "$cw\HOLCto1940.dta" /*Crosswalk file*/
keep if _merge == 3
drop _merge
```

2. For variables expressed as counts, simply weight them with the areal weight ch1940 (share of the 1940 tract that falls in the HOLC graded neighborhood)

```
local varlist "white population"
foreach var of local varlist{
    gen wt`var' = `var'*ch1940
}
```

3. For variables expressed as counts, add the weighted observations of the previous step at the HOLC neighborhood level

```
local varlist "white population"
foreach var of local varlist{
    bysort index: egen `var'1940 = total(wt`var'), missing
}
```

4. Generate the variable of interest, drop duplicates and save

```
gen WhiteShare1940 = white1940/population1940
keep index WhiteShare1940 population1940
egen tag = tag(index)
keep if tag
save "$data\population1940.dta", replace
```

5. For home values and income, after obtaining the MSA medians, apply the crosswalks to the number of housing units or families in each interval, attach the midpoint of the

interval or the value if its the first or last reported interval and compute the share on and above the MSA median for each graded neighborhood.

6. For variables reported as means, apply the crosswalks to the relevant count variable, attach the value and obtain the mean in the polygon. For instance, for average family income obtain the cross-walked number of families, multiply it by the reported income and average it for each neighborhood.

9.2 Waterfront modifications data sources

In this appendix, I describe the waterfront modifications that were considered together with their data source. Details on reasons why some cities are not considered here as well as additional information can be made available upon request. These modifications have been merged to a single shapefile that is also available upon request⁵⁷.

Baltimore: Data for waterfront improvements comes directly from the digitized Urban Renewal Plans of the Baltimore Department of Planning. The date for the Canton Waterfront comes from the same plan, which was approved in 1984. By establishing the date to be 1990, the modification taking into account the date will only appear from 2000 onward, giving a long enough time window for it to have been taken place. For Inner Harbor, the project was approved in 1967, the date chosen is because in 1976 a series of celebrations of the US Bicentennial took place there, suggesting the project had already been, at least partially, completed.

Boston: Boston Waterfront modifications include the creation of the Christopher Columbus Waterfront Park and the Harborwalk. The location of the first one comes from selecting that park from the Open Space shapefile provided by the City of Boston Open data portal. The area is meant to capture the waterfront and the redevelopment of Faneuil Hall area. The Harborwalk is obtained extracting it from the shapefile containing shared walker trails from the following dataset. Dates are based on the New York's Time Article "*BOSTON WATERFRONT: AT 25, A MODEL URBAN RENEWAL*" (1986) available [here](#).

Bronx: All data comes from the New York City Departments of Parks and & Recreation. The parks are extracted from the Open Space Recreation Parks shapefile provided by the City of New York. The Bronx River Greenway is obtained merging the Bronx Park and the Shoelace since no park with such name appeared on the shapefile.

Brooklyn: Data for the Brooklyn Bridge Park is obtained in the same way as the data for Bronx. Only the completed parts of the Brooklyn Waterfront Greenway are considered. They are obtained extracting the objects designed as greenway from the New York Biking Routes shapefile and comparing them to the ones provided by the Brooklyn Greenway Initiative (BGI). The attached date is based on the information given by the BGI.

Buffalo: Although the waterfront redevelopment of Buffalo is not considered in the analysis because the buffer around it does not intersect any graded neighborhood, the modification considered is the redevelopment of Canalside. It was geolocated with the coordinates of Canalside on Google Maps. The attached date was 2008, when the Central Wharf was inaugurated. More information can be found [here](#).

Cambridge: The modifications considered come from the Cambridge Community Development Department. It considers the 1978 East Cambridge Riverfront Plan and the 1983 Cambridgeport Revitalization Plan. It was geolocated by extracting the districts of East Waterfront and Cambridgeport.

Chicago: Modifications considered include the Riverwalk and the Lake Front Trail. The information of the Riverwalk was obtained from the Chicago River Timeline from the Chicago River Edge Ideas Lab which depends on the City of Chicago's Department of Planning and

⁵⁷For some areas, it was unclear whether if a modification had taken place or not and there were incongruities among data sources. As a result, I only considered the modifications that according to the majority of data sources had been fully implemented and, in case of doubt, by inspecting the area in Google Street View and comparing it to the rest of the areas before deciding.

Development. It was geolocated with the Open Spaces-Riverwalk shapefile of the Chicago Data Portal. The date is chosen because it was when the construction between Lake Shore Drive and Michigan Avenue started. Data on the Lake Front Trail is extracted similarly from the Bike Routes of the Chicago Data Portal. It was designated as a bike trial in 1963.

Columbus: The considered modifications were extracted because of their appearance in the case study by the City of Columbus and MKSK studios, which can be accessed here. The created parks (Genoa Park, Lower Scioto Park and North Bank Park) were extracted from the City of Columbus Open Data Park Property Boundaries shapefile. The buffer around the North Bank Park does not intersect with neighborhoods and hence it does not appear in Appendix Table 9.3.8.

Duluth: only consideres the Canal Park. It was chosen because of the Duluth New Tribune 2010 Article "*History: Changing Duluth's waterfront from junk to jewel of the North*", accessible here. It was geolocated by extracting all addressed structures in Canal Park from the Adress Point shapefile of the St. Luois County (MN) data portal.

Indianapolis: information on Canal Walk was obtained from the Cultural Landscape Foundation. It was geolocated by extracting the objects named Canal Walk from the Indianapolis Parks shapefile provided by the City of Indianapolis data portal.

Louisville: Information for the Waterfront Park was obtained from its web page. It was located by extracting the areas named Waterfront Park from the Luoisville Metro Areas of Interest shapefile of the Louisvile Open Geospatial Data portal.

Lower Westchester County: The only modification is a part of the Bronx River Parkway that intersects one neighborhood there. See description for Bronx.

Manhattan: Considered parks were extracted following the New York City Comprehensive Waterfront Plan (1992) and the Vision 2020: New York City Comprehensive Waterfront Park (2011). They are all extracted from the Open Space shapefile of the NYC data portal.

Minneapolis: Nicollet Island was deemed as a modification following this newspaper article. Even if other areas could have been relevant (i.e., Hennepin Island, Promenade Main Street, West Bank Waterfront, Basett's creek) I was only able to locate Nicollet Island extracting the parks with such name from Minneapolist Open Data. Moreover, using google street view these areas, as well as the riverbank, did not seem to have been developed in a comparable way to other areas in other cities.

New Orleans: although it does not intersect any neighborhood, the modifications considered were the ones that took place around the French Quarters (Moonwalk and Woldbenger Park). They were located by extracting them from the Parks data of New Orleans.

Philadelphia: Penn's Landing was considered because of the mentions in Visit Philly tourism web page. It was located by extracting the parks that would correspond to its location according to Google Maps, which would include the Irish Memorial, the Korean War Veteran's Memorial and the Vietnam Memorial. The date was chosen since it was the inauguration of Penn's Landing Great Plaza.

Pittsburgh: The parks located are the ones that belong to the Three Rivers Parks (Monongahela, Allegheny and Ohio) following the Pittsburgh Waterfront Master Plan. The dates and specific parks were extracted from the Pittsburgh nonprofit organization Riverlife. Besides the ones on Appendix Table 9.3.8, the Point State Park and the Northshore Riverfront Park were also considered but they do not intersect any neighborhood.

Portland: Following Portland's Park and Recreation Department, the only two considered features were the South Waterfront Park, which includes the Gov. Tom McCall Waterfront Park, and the Vera Katz Eastbank Esplanade. They were located by extracting these features from parks shapefiles.

Seattle: The modifications considered to capture the Seattle waterfront redevelopment were the location of the Aquarium and the Waterfront Park. However, the buffers around them do not intersect any neighborhood.

Queens: The sole modification is a part of the Brooklyn Bridge Park that intersects neighborhoods in Queens. See Brooklyn.

9.3 Additional evidence and results

Figure 9.3.1: Predicted Tree Canopy in Manhattan (2006)



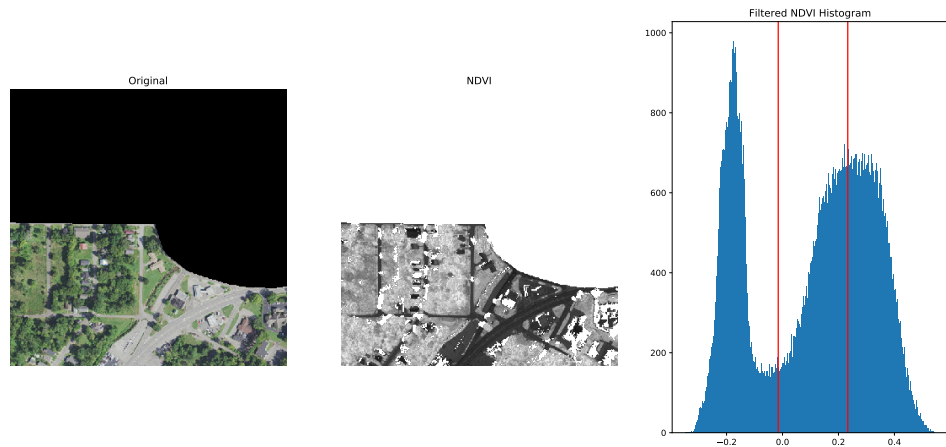
Notes: This image shows the predicted tree pixels obtained with the methodology described in Section 3 for an area in Manhattan in 2006 (green) and 2015 (pink). The ground image corresponds to the 2006 NAIP image. Colors have been equalized to the 2015 reference. Source: NAIP Imagery. Own elaboration.

Figure 9.3.2: Predicted Tree Canopy in Manhattan (2015)



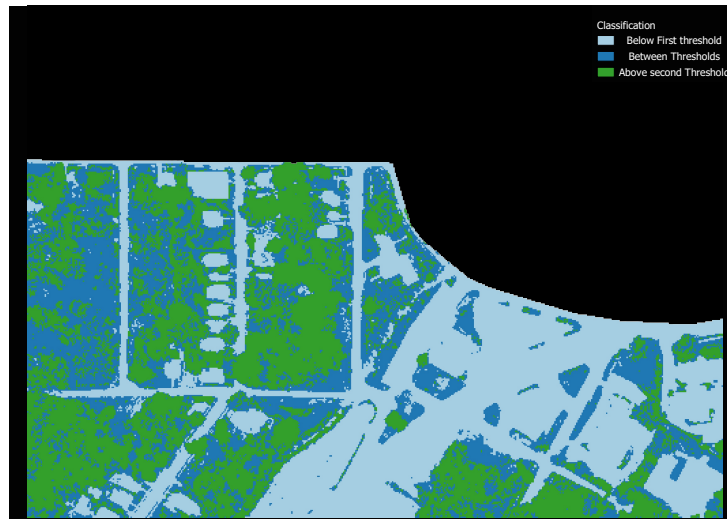
Notes: This image shows the predicted tree pixels obtained with the methodology described in Section 3 for an area in Manhattan in 2006 (green) and 2015 (pink). The ground image corresponds to the 2015 NAIP image. Source: NAIP Imagery. Own elaboration.

Figure 9.3.3: Otsu's Double Thresholding Algorithm



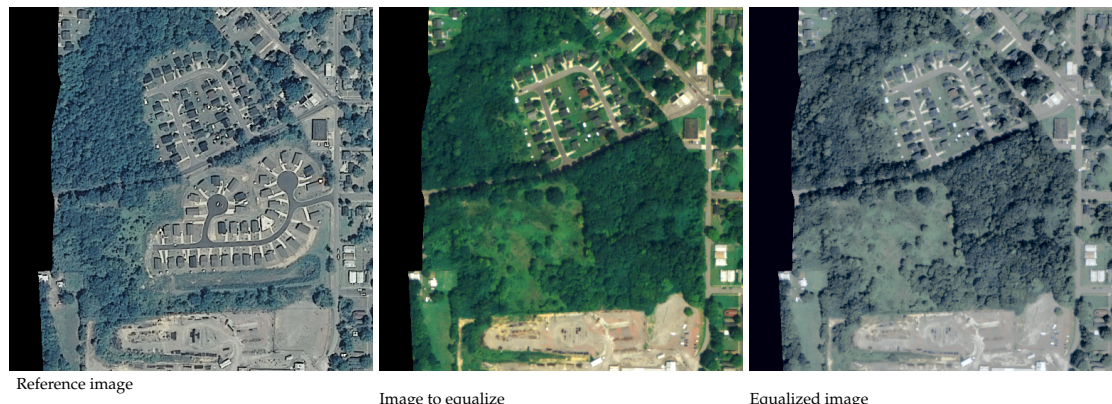
Notes: This image illustrates the functioning of Otsu's double thresholding algorithm. The figure on the left represents the original NAIP image. The middle figure represents the NDVI value for each pixel, with higher values depicted lighter. The figure on the right represents the histogram of the smoothed NDVI values and the two thresholds obtained with Otsu's thresholding. Source: NAIP Imagery. Own elaboration.

Figure 9.3.4: Otsu's Double Thresholding Algorithm



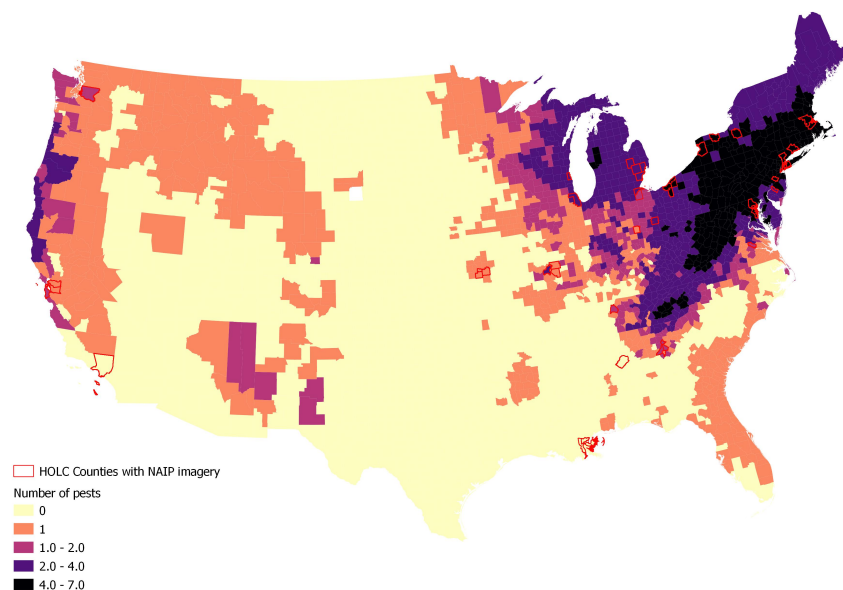
Notes: This image represents how pixels in the original image of Figure 9.3.3 are classified after applying Otsu's double thresholding. Source: NAIP Imagery. Own elaboration.

Figure 9.3.5: Color equalization



Notes: This image shows the results of applying lightness and color histogram matching. The reference image (left) is the NAIP image when NIR data is available. The middle image is the same area for the first data period, with no NIR data. The image on the right shows the first period image after applying histogram matching to equalize its colors to the reference image. Source: NAIP imagery. Own elaboration.

Figure 9.3.6: County distribution of pests



Notes: This image shows the county distribution of the total number of deadliest non-native pests. Source: Fei et al. (2019). Own elaboration.

Figure 9.3.7: Total pests hosts species



Notes: This image shows the distribution of potential hosts species for the deadliest plagues. Source: Fei et al. (2019) and Wilson et al. (2013). Own elaboration.

Table 9.3.1: Distribution of grades and neighborhoods per decade

	Number of neighborhoods		
	No natural amenities	Natural amenities	Total
A-Green	131	233	364
B-Blue	347	540	887
C-Yellow	602	880	1482
D-Red	348	603	951
Total	1428	2256	3684

Notes: This table shows the number of neighborhoods with Census data considered every decade.

Source: see data description. Own elaboration.

Table 9.3.2: Population distribution, 1940

	Population Share	White Share	Black Share
A-Green	0.03	0.03	0.01
B-Blue	0.16	0.18	0.02
C-Yellow	0.41	0.44	0.10
D-Red	0.40	0.35	0.87

Notes: This table shows the share of sample population living in each kind of graded neighborhood in 1940.

Source: see data description. Own elaboration.

Table 9.3.3: Summary Statistics, 1940

	Black Share	White Share	% HU above MSA Median Value
A-Green			
Mean	0.02	0.98	0.89
Std. Dev	0.04	0.04	0.13
B-Blue			
Mean	0.02	0.98	0.79
Std. Dev	0.05	0.05	0.16
C-Yellow			
Mean	0.03	0.97	0.63
Std. Dev	0.08	0.08	0.20
D-Red			
Mean	0.13	0.87	0.43
Std. Dev	0.22	0.22	0.21
Total			
Mean	0.05	0.95	0.64
Std.Dev	0.13	0.13	0.24

Notes: This table shows summary statistics for each variable and grade in 1940. Family income is not considered because it is only available from 1950.

Source: see data description. Own elaboration.

Table 9.3.4: Summary Statistics, 2015

	Black Share	White Share	% HU above MSA Median Value	% Familes above above MSA Median Income
A-Green				
Mean	0.16	0.72	0.75	0.72
Std.Dev.	0.26	0.26	0.28	0.18
B-Blue				
Mean	0.23	0.62	0.57	0.56
Std.Dev	0.31	0.30	0.33	0.22
C-Yellow				
Mean	0.31	0.51	0.45	0.42
Std. Dev	0.34	0.31	0.31	0.21
D-Red				
Mean	0.38	0.44	0.39	0.35
Std. Dev	0.34	0.29	0.30	0.21
Total				
Mean	0.29	0.54	0.49	0.46
Std. Dev	0.33	0.31	0.33	0.24

Notes: This table shows summary statistics for each variable and grade in 2015.

Source: see data description. Own elaboration.

Table 9.3.5: Descriptive statistics for tree canopy.

	% Tree Pixels 2000	% Tree Pixels 2015	Δ TC
A-Green			
Mean	0.26	0.28	0.63
Std. Dev.	0.13	0.12	3.17
B-Blue			
Mean	0.22	0.25	0.43
Std. Dev.	0.13	0.12	1.29
C-Yellow			
Mean	0.18	0.21	0.64
Std. Dev.	0.12	0.10	1.76
D-Red			
Mean	0.16	0.18	0.78
Std. Dev.	0.12	0.11	2.10
Total			
Mean	0.19	0.22	0.63
Std.Dev	0.12	0.11	1.95

Notes: This table shows summary statistics for percentage of tree pixels in 2000 and 2015 and its growth rate between 2000s-2015 .

Source: see data description. Own elaboration.

Table 9.3.6: Redlined cities and corresponding 2010 MSA

2010 MSA/CBSA	HOLC City	Neighborhoods	%
Akron, OH	Akron	495.0	1.5
Atlanta-Sandy Springs-Marietta, GA	Atlanta	1,089.0	3.3
Baltimore-Towson, MD	Baltimore	405.0	1.2
Birmingham-Hoover, AL	Birmingham	279.0	0.8
Boston-Cambridge-Quincy, MA-NH	Boston	351.0	1.1
Boston-Cambridge-Quincy, MA-NH	Cambridge	135.0	0.4
Boston-Cambridge-Quincy, MA-NH	Somerville	9.0	0.0
Buffalo-Niagara Falls, NY	Buffalo	342.0	1.0
Chicago-Joliet-Naperville, IL-IN-WI	Chicago	3,006.0	9.1
Cleveland-Elyria-Mentor, OH	Cleveland	1,755.0	5.3
Columbus, OH	Columbus	540.0	1.6
Dallas-Fort Worth-Arlington, TX	Dallas	234.0	0.7
Dayton, OH	Dayton	396.0	1.2
Denver-Aurora-Broomfield, CO	Denver	477.0	1.4
Detroit-Warren-Livonia, MI	Detroit	2,097.0	6.3
Duluth, MN-WI	Duluth	306.0	0.9
Flint, MI	Flint	477.0	1.4
Indianapolis-Carmel, IN	Indianapolis	792.0	2.4
Kansas City, MO-KS	Greater Kansas City	468.0	1.4
Los Angeles-Long Beach-Santa Ana, CA	Los Angeles	3,978.0	12.0
Louisville/Jefferson County, KY-IN	Louisville	324.0	1.0
Milwaukee-Waukesha-West Allis, WI	Milwaukee Co.	432.0	1.3
Minneapolis-St. Paul-Bloomington, MN-WI	Minneapolis	765.0	2.3
Nashville-Davidson-Murfreesboro-Franklin, TN	Nashville	9.0	0.0
New Haven-Milford, CT	New Haven	234.0	0.7
New Orleans-Metairie-Kenner, LA	New Orleans	1,071.0	3.2
New York-Northern New Jersey-Long Island, NY-NJ-PA	Bronx	405.0	1.2
New York-Northern New Jersey-Long Island, NY-NJ-PA	Brooklyn	603.0	1.8
New York-Northern New Jersey-Long Island, NY-NJ-PA	Lower Westchester Co.	441.0	1.3
New York-Northern New Jersey-Long Island, NY-NJ-PA	Manhattan	477.0	1.4
New York-Northern New Jersey-Long Island, NY-NJ-PA	Queens	1,548.0	4.7
New York-Northern New Jersey-Long Island, NY-NJ-PA	Staten Island	648.0	2.0
New York-Northern New Jersey-Long Island, NY-NJ-PA	Philadelphia	180.0	0.5
Philadelphia-Camden-Wilmington, PA-NJ-DE-MD	Camden	666.0	2.0
Philadelphia-Camden-Wilmington, PA-NJ-DE-MD	Pittsburgh	1,026.0	3.1
Pittsburgh, PA	Portland	909.0	2.7
Portland-Vancouver-Hillsboro, OR-WA	Richmond	387.0	1.2
Richmond, VA	Rochester	288.0	0.9
Rochester, NY	Oakland	1,278.0	3.9
San Francisco-Oakland-Fremont, CA	San Francisco	945.0	2.9
San Francisco-Oakland-Fremont, CA	Seattle	540.0	1.6
Seattle-Tacoma-Bellevue, WA	East St. Louis	315.0	1.0
St. Louis, MO-IL	St.Louis	1,233.0	3.7
St. Louis, MO-IL	Syracuse	378.0	1.1
Syracuse, NY	Toledo	351.0	1.1
Toledo, OH	Trenton	72.0	0.2
Total		33,156.0	100.0

Notes: This table shows the total number of neighborhoods with Census data (1940-2015) for each HOLC city and their corresponding MSA. Differences in the amount of neighborhoods per city are due to the geographic variation of 1940 tract coverage, across the US and within cities, and to differences in population location within cities that resulted into a different number of areas being surveyed by the HOLC as neighborhoods.

Source: see data description. Own elaboration.

Table 9.3.7: Redlined cities and NAIP Imagery

2010 MSA/CBSA	HOLC City	First NAIP image year	Second NAIP image year
Akron, OH	Akron	2004	2015
Atlanta-Sandy Springs-Marietta, GA	Atlanta	2007	2015
Baltimore-Towson, MD	Baltimore	2005	2015
Birmingham-Hoover, AL	Birmingham	2006	2015
Boston-Cambridge-Quincy, MA-NH	Boston	2003	2014
Boston-Cambridge-Quincy, MA-NH	Cambridge	2003	2014
Boston-Cambridge-Quincy, MA-NH	Somerville	2003	2014
Buffalo-Niagara Falls, NY	Buffalo	2006	2015
Chicago-Joliet-Naperville, IL-IN-WI	Chicago	2007	2015
Cleveland-Elyria-Mentor, OH	Cleveland	2004	2015
Columbus, OH	Columbus	2004	2015
Dayton, OH	Dayton	2004	2015
Detroit-Warren-Livonia, MI	Detroit	2005	2014
Flint, MI	Flint	2005	2014
Kansas City, MO-KS	Greater Kansas City	2007	2015
Los Angeles-Long Beach-Santa Ana, CA	Los Angeles	2005	2014
Milwaukee-Waukesha-West Allis, WI	Milwaukee Co.	2005	2015
Nashville-Davidson-Murfreesboro-Franklin, TN	Nashville	2006	2014
New Haven-Milford, CT	New Haven	2006	2014
New Orleans-Metairie-Kenner, LA	New Orleans	2007	2015
New York-Northern New Jersey-Long Island, NY-NJ-PA	Bronx	2006	2015
New York-Northern New Jersey-Long Island, NY-NJ-PA	Brooklyn	2006	2015
New York-Northern New Jersey-Long Island, NY-NJ-PA	Lower Westchester Co.	2006	2015
New York-Northern New Jersey-Long Island, NY-NJ-PA	Manhattan	2006	2015
New York-Northern New Jersey-Long Island, NY-NJ-PA	Queens	2006	2015
New York-Northern New Jersey-Long Island, NY-NJ-PA	Staten Island	2006	2015
New York-Northern New Jersey-Long Island, NY-NJ-PA	Camden	2006	2015
Philadelphia-Camden-Wilmington, PA-NJ-DE-MD	Richmond	2003	2015
	Rochester	2006	2015
	Oakland	2005	2014
San Francisco-Oakland-Fremont, CA	San Francisco	2005	2014
San Francisco-Oakland-Fremont, CA	Seattle	2006	2015
Seattle-Tacoma-Bellevue, WA	East St. Louis	2007	2015
St. Louis, MO-IL	St.Louis	2007	2015
St. Louis, MO-IL	Syracuse	2006	2015
Syracuse, NY	Toledo	2004	2015
Toledo, OH	Trenton	2006	2015
Trenton-Ewing, NJ			

Notes: This table shows the cities with available NAIP imagery and the two years years considered to predict tree canopy

Source: see data description. Own elaboration.

Table 9.3.8: Geolocated waterfront modifications

HOLC city	Modification	Date
Baltimore	Canton Waterfront	1990
Baltimore	Inner Harbor East	1976
Baltimore	Inner Harbor Project I	1976
Boston	Harborwalk	1984
Boston	Waterfront	1976
Bronx	Bronx Park	2000
Bronx	Bronx River Parkway	2000
Bronx	Hunts Point Riverside Park	2007
Bronx	Sherman Creek	2003
Brooklyn	Brooklyn Bridge Park	2010
Brooklyn	Brooklyn Greenway	2010
Cambridge	Cambridgeport	1983
Cambridge	East Cambridge	1978
Chicago	Lakefront Trail	1963
Chicago	Riverwalk	2001
Columbus	Genoa Park	1999
Columbus	Lower Scioto Park	2009
Duluth	Canal Park, Duluth	1993
Indianapolis	Canal Walk, Indianapolis	2001
Louisville	Waterfront park, Louisville	1999
Lower Westchester Co.	Bronx River Parkway	2000
Manhattan	Manhattan Greenway	1999
Manhattan	Nutter's Battery & Fort Clinton Site	2001
Manhattan	Riverside Park	1981
Manhattan	Sherman Creek	2003
Minneapolis	Nicolett Island	1983
Philadelphia	Penn's Landing	1986
Pittsburgh	Allegheny Landing Park	2000
Pittsburgh	Monongahela Wharf Landing Park	2009
Pittsburgh	Southside Riverfront Park	2012
Pittsburgh	Washington's Landing Park	1980
Portland	Gov Tom McCall Waterfront Park	1978
Portland	Vera Katz Eastbank Esplanade	2000
Queens	Brooklyn Bridge Park	2010

Notes: This table shows the geolocated modifications, their date and the corresponding HOLC city.

Source: see data description and Appendix 9.2. Own elaboration.

Table 9.3.9: Within MSA persistence of redlining, 1980

VARIABLES	(1)	(2)	(3)
	White Share	% HU above MSA MHV	% Families above MSA MFI
D-graded	-0.140*** (0.00634)	-0.182*** (0.00563)	-0.115*** (0.00341)
D-graded \times Post ¹⁹⁷⁷	0.0246* (0.0149)	0.0568*** (0.0117)	0.0255** (0.00699)
Observations	9,732	9,698	9,730
Year FE	YES	YES	YES
MSA FE	YES	YES	YES
Border-pair FE	NO	NO	NO
Sample	All D-C	All D-C	All D-C
Adjusted Within R-squared	0.0554	0.105	0.127
Mean Dep. Var	0.635	0.409	0.429

Robust standard errors in parentheses

*** p<0.01, ** p<0.05, * p<0.1

Notes: This table shows the results of estimating Equation 1 using the entire D-C sample. Post¹⁹⁷⁷ is restricted 1980.
All variables are described as in the text.HU: stands for housing units, MHV for median house vale and MFI for median family income.

Table 9.3.10: Within D-C pair persistence of redlining, 1980

VARIABLES	(1)	(2)	(3)
	White Share	% HU above MSA MHV	% Families above MSA MFI
D-graded	-0.0847*** (0.00547)	-0.0946*** (0.00465)	-0.0593*** (0.00272)
D-graded \times Post ¹⁹⁷⁷	0.0367*** (0.0123)	0.0493*** (0.0102)	0.0211*** (0.00543)
Observations	4,816	4,813	4,816
Year FE	YES	YES	YES
MSA FE	Absorbed	Absorbed	Absorbed
Border-pair FE	YES	YES	YES
Sample	Bordering D-C	Bordering D-C	Bordering D-C
Adjusted Within R-squared	0.0543	0.0899	0.114
Mean Dep. Var	0.592	0.344	0.390

Robust standard errors in parentheses

*** p<0.01, ** p<0.05, * p<0.1

Notes: This table shows the results of estimating Equation 1 using the bordering D-C sample. Post¹⁹⁷⁷ is restricted 1980. All variables are described as in the text.HU: stands for housing units, MHV for median house vale and MFI for median family income.

Table 9.3.11: Placebo

VARIABLES	(1) White Share	(2) % HU above MSA MHV	(3) % Families above MSA MFI
Placebo D-graded	-0.00582 (0.0115)	0.00304 (0.0109)	0.00156 (0.00598)
Natural Amenities	-0.0162 (0.0121)	-0.0353*** (0.0116)	-0.0200*** (0.00690)
Placebo D-graded × Natural Amenities	0.00350 (0.0149)	0.00528 (0.0142)	0.00341 (0.00824)
Placebo D-graded × <i>Post</i> ¹⁹⁷⁷	0.00450 (0.0128)	-0.00477 (0.0123)	0.00633 (0.00711)
Natural Amenities × <i>Post</i> ¹⁹⁷⁷	0.0267** (0.0118)	0.0464*** (0.0115)	0.0317*** (0.00685)
Placebo D-graded × Natural Amenities × <i>Post</i> ¹⁹⁷⁷	0.00851 (0.0163)	0.00289 (0.0158)	-0.00599 (0.00954)
Observations	9,632	9,629	9,632
Year FE	YES	YES	YES
MSA FE	Absorbed	Absorbed	Absorbed
Border-pair FE	YES	YES	YES
Sample	Bordering D-C	Bordering D-C	Bordering D-C
Adjusted Within R-squared	0.00160	0.00421	0.00395
Mean Dep. Var	0.592	0.344	0.390

Robust standard errors in parentheses

*** p<0.01, ** p<0.05, * p<0.1

Notes: This table shows the results from estimating Equation 2 using placebo grades. Placebo grades (D or C) are assigned to originally D areas, then the adjacent C area is assigned the opposite grade.

Table 9.3.12: Natural-amenities year fixed effects, within MSA

VARIABLES	(1) White Share	(2) % HU above MSA MHV	(3) % Families above MSA MFI
D-graded	-0.133*** (0.0104)	-0.135*** (0.00978)	-0.0945*** (0.00576)
Natural Amenities	0.0114 (0.00775)	0.0131 (0.0113)	0.00910 (0.00601)
D-graded \times Natural Amenities	-0.0189 (0.0131)	-0.0711*** (0.0122)	-0.0286*** (0.00722)
D-graded \times Post ¹⁹⁷⁷	0.0589*** (0.0138)	0.0706*** (0.0125)	0.0267*** (0.00772)
D-graded \times Natural Amenities \times Post ¹⁹⁷⁷	-0.00900 (0.0174)	0.0368** (0.0157)	0.00819 (0.00978)
Observations	19,460	19,418	19,454
Year FE	YES	YES	YES
MSA FE	YES	YES	YES
Border-pair FE	NO	NO	NO
Amenities- Year FE	YES	YES	YES
Sample	All D-C	All D-C	All D-C
Adjusted Within R-squared	0.0366	0.0560	0.0726
Mean Dep. Var	0.635	0.409	0.429

Robust standard errors in parentheses

*** p<0.01, ** p<0.05, * p<0.1

Notes: This table shows the results from estimating Equation 2 and adding geography-year fixed effects at the MSA level. All variables are defined as in the text.

Table 9.3.13: Natural-amenities year fixed effects, within D-C pair

VARIABLES	(1) White Share	(2) % HU above MSA MHV	(3) % Families above MSA MFI
D-graded	-0.0781*** (0.0112)	-0.0761*** (0.0106)	-0.0512*** (0.00574)
Natural Amenities	-0.0218 (0.0162)	-0.0290* (0.0160)	-0.0148 (0.00937)
D-graded × Natural Amenities	-0.0110 (0.0145)	-0.0309** (0.0138)	-0.0136* (0.00793)
D-graded × <i>Post</i> ¹⁹⁷⁷	0.0270** (0.0125)	0.0399*** (0.0120)	0.0140** (0.00687)
D-graded × Natural Amenities × <i>Post</i> ¹⁹⁷⁷	0.0274* (0.0160)	0.0297* (0.0154)	0.00761 (0.00923)
Observations	9,632	9,629	9,632
Year FE	YES	YES	YES
MSA FE	Absorbed	Absorbed	Absorbed
Border-pair FE	YES	YES	YES
Amenities- Year FE	YES	YES	YES
Sample	Bordering D-C	Bordering D-C	Bordering D-C
Adjusted Within R-squared	0.0327	0.0378	0.0513
Mean Dep. Var	0.592	0.344	0.390

Robust standard errors in parentheses

*** p<0.01, ** p<0.05, * p<0.1

Notes: This table shows the results from estimating Equation 2 and adding geography-year fixed effects at the D-C pair level. All variables are defined as in the text.

Table 9.3.14: Alternative to capture natural amenities

VARIABLES	(1) White Share	(2) % HU above MSA MHV	(3) % Families above MSA MFI
D-graded	-0.0798*** (0.0120)	-0.0689*** (0.0109)	-0.0513*** (0.00614)
Natural Amenities	-0.00726 (0.0117)	-0.0206* (0.0108)	-0.0108* (0.00630)
D-graded \times Natural Amenities	-0.00751 (0.0147)	-0.0398*** (0.0139)	-0.0123 (0.00820)
D-graded \times Post ¹⁹⁷⁷	0.0407*** (0.0133)	0.0387*** (0.0123)	0.0161** (0.00727)
Natural Amenities \times Post ¹⁹⁷⁷	0.0432*** (0.0117)	0.0606*** (0.0107)	0.0336*** (0.00644)
D-graded \times Natural Amenities \times Post ¹⁹⁷⁷	0.00331 (0.0164)	0.0284* (0.0155)	0.00294 (0.00939)
Observations	9,632	9,629	9,632
Year FE	YES	YES	YES
MSA FE	Absorbed	Absorbed	Absorbed
Border-pair FE	YES	YES	YES
Sample	Bordering D-C	Bordering D-C	Bordering D-C
Adjusted Within R-squared	0.0367	0.0487	0.0565
Mean Dep. Var	0.592	0.344	0.390

Robust standard errors in parentheses

*** p<0.01, ** p<0.05, * p<0.1

Notes: This table shows the results from estimating Equation 2 using a different definition of natural amenities. Natural amenities are defined as a situation when the share of the neighborhood covered by the buffer around water and parks is greater than the median for the MSA. The rest of variables are defined as in the text.

Table 9.3.15: Modifying natural amenities, alternative definition of modifications

VARIABLES	(1) White Share	(2) % HU above MSA MHV	(3) % Families above MSA MFI
D-graded	-0.133*** (0.0104)	-0.136*** (0.00975)	-0.0947*** (0.00576)
Natural Amenities	0.0231*** (0.00670)	0.0240*** (0.00780)	0.00851** (0.00402)
D-graded × Natural Amenities	-0.0186 (0.0131)	-0.0705*** (0.0122)	-0.0284*** (0.00722)
D-graded × <i>Post</i> ¹⁹⁷⁷	0.0589*** (0.0138)	0.0706*** (0.0125)	0.0268*** (0.00772)
Natural Amenities × <i>Post</i> ¹⁹⁷⁷	0.0346*** (0.00989)	0.0161 (0.0101)	0.0187*** (0.00568)
Natural Amenities × Modification × <i>Post</i> ¹⁹⁷⁷	0.0379 (0.0249)	0.173*** (0.0220)	0.00392 (0.0189)
D-graded × Natural Amenities × <i>Post</i> ¹⁹⁷⁷	-0.0155 (0.0174)	0.0290* (0.0157)	0.00323 (0.00980)
D-graded × Natural Amenities × Modification × <i>Post</i> ¹⁹⁷⁷	0.0906*** (0.0317)	0.0530* (0.0286)	0.0813*** (0.0250)
Observations	19,460	19,418	19,454
Year FE	YES	YES	YES
MSA FE	YES	YES	YES
Border-pair FE	NO	NO	NO
Sample	All D-C	All D-C	All D-C
Adjusted Within R-squared	0.0416	0.0661	0.0759
Mean Dep. Var	0.635	0.409	0.429

Robust standard errors in parentheses

*** p<0.01, ** p<0.05, * p<0.1

Notes: This table shows the results from estimating a modified version of Equation 3 on the MSA D-C sub-sample, for the period 1950-2015. Modification takes value one only for those neighborhoods that fall within the 500m buffer around them and after the modification has taken place. *Post*¹⁹⁷⁷ is defined from 1980-2015. Natural amenities and modifications are described as in the text.

Table 9.3.16: Modifying natural amenities, excluding parks

VARIABLES	(1) White Share	(2) % HU above MSA MHV	(3) % Families above MSA MFI
D-graded	-0.154*** (0.00738)	-0.170*** (0.00653)	-0.114*** (0.00399)
Natural Amenities	0.0121 (0.00776)	0.0138 (0.0110)	0.0100* (0.00529)
D-graded × Natural Amenities	0.0397*** (0.0146)	-0.0311** (0.0155)	0.00954 (0.00845)
Natural Amenities × Modification	0.0605*** (0.0183)	-0.0120 (0.0343)	-0.0265* (0.0152)
D-graded × Natural Amenities × Modification	0.0228 (0.0265)	-0.0820* (0.0465)	-0.0227 (0.0231)
D-graded × Post ¹⁹⁷⁷	0.0545*** (0.00964)	0.0910*** (0.00847)	0.0307*** (0.00535)
Natural Amenities × Post ¹⁹⁷⁷	0.0567*** (0.0121)	0.0294** (0.0141)	0.0114 (0.00774)
Natural Amenities × Modification × Post ¹⁹⁷⁷	-0.0566* (0.0341)	0.0687 (0.0427)	-0.00899 (0.0249)
D-graded × Natural Amenities × Post ¹⁹⁷⁷	-0.0290 (0.0203)	-0.0207 (0.0200)	-0.0112 (0.0121)
D-graded × Natural Amenities × Modification × Post ¹⁹⁷⁷	0.109** (0.0435)	0.150*** (0.0578)	0.113*** (0.0350)
Observations	19,460	19,418	19,454
Year FE	YES	YES	YES
MSA FE	YES	YES	YES
Border-pair FE	NO	NO	NO
Sample	All D-C	All D-C	All D-C
Adjusted Within R-squared	0.0457	0.0578	0.0737
Mean Dep. Var	0.635	0.409	0.429

Robust standard errors in parentheses

*** p<0.01, ** p<0.05, * p<0.1

Notes: This table shows the results from estimating Equation 3 on the MSA D-C sub-sample, for the period 1950-2015. Natural amenities are defined only with water features and modifications are described as in the text.

Table 9.3.17: Reduced form results

VARIABLES	(1)	(2)	(3)
	White Share	% HU above MSA MHV	% Families above MSA MFI
D-graded	-0.0858*** (0.0250)	-0.0365* (0.0190)	-0.0864*** (0.0155)
Δ Plague Exposure	2.472* (1.369)	-0.604 (0.704)	0.925 (0.880)
D-graded × Δ Plague Exposure	25.92*** (9.364)	5.328 (7.393)	15.78*** (5.773)
Interpretation:			
D × Δ 1 SD Δ Plague Exposure	0.14	0.029	0.088
Observations	1,384	1,383	1,384
MSA FE	YES	YES	YES
D x NA	YES	YES	YES
D x NA x Modification	YES	YES	YES
Sample	All D-C in 2015	All D-C in 2015	All D-C in 2015
Adjusted Within R-squared	0.0333	0.0127	0.0563
Mean Dep. Var	0.444	0.380	0.366

Robust standard errors in parentheses

*** p<0.01, ** p<0.05, * p<0.1

Notes: This table shows the results from estimating a reduced form Equation 4 with changes in plague exposure on the MSA D-C sample. Changes in tree canopy cover the period 2000s-2015. All variables are defined as in the text. Due to the inaccuracy of tree canopy predictions in Los Angeles, Oakland, San Francisco and Chicago, these cities are excluded from the regression.

Table 9.3.18: Second stage

VARIABLES	(1)	(2)	(3)
	White Share	% HU above MSA MHV	% Families above MSA MFI
Panel A: OLS			
D-graded	-0.0689*** (0.0259)	-0.0402** (0.0190)	-0.0828*** (0.0166)
ΔTC	0.0128*** (0.00443)	0.0114** (0.00463)	-0.00110 (0.00525)
D-graded $\times \Delta TC$	-0.00736 (0.00922)	0.00806 (0.00696)	0.00748 (0.0100)
Adjusted Within R-squared	0.0246	0.0249	0.0493
Panel B: TSLS			
D-graded	-0.354*** (0.102)	-0.0901 (0.0813)	-0.249*** (0.0630)
$\widehat{\Delta TC}$	0.0477* (0.0264)	-0.0116 (0.0136)	0.0178 (0.0170)
D-graded $\times \widehat{\Delta TC}$	0.438*** (0.161)	0.0924 (0.127)	0.268*** (0.0990)
Observations	1,384	1,383	1,384
MSA FE	YES	YES	YES
D x NA	YES	YES	YES
D x NA x Modification	YES	YES	YES
Sample	All D-C in 2015	All D-C in 2015	All D-C in 2015
Adjusted Within R-squared	0.0333	0.0127	0.0563
Mean Dep. Var	0.444	0.380	0.366

Robust standard errors in parentheses

*** p<0.01, ** p<0.05, * p<0.1

Notes: This table shows the results from estimating a reduced form Equation 4 with changes in plague exposure on the MSA D-C sample. Changes in tree canopy cover the period 2000s-2015. All variables are defined as in the text. Due to the inaccuracy of tree canopy predictions in Los Angeles, Oakland, San Francisco and Chicago, these cities are excluded from the regression.